Integration of nitrogen cycle dynamics into the Integrated Science Assessment Model for the study of terrestrial ecosystem responses to global change

Xiaojuan Yang,[1] Victoria Wittig,[1] Atul K. Jain,[1] and Wilfred Post[2]

Received 20 January 2009; revised 4 August 2009; accepted 13 August 2009; published 30 December 2009.

[1] A comprehensive model of terrestrial N dynamics has been developed and coupled with the geographically explicit terrestrial C cycle component of the Integrated Science Assessment Model (ISAM). The coupled C-N cycle model represents all the major processes in the N cycle and all major interactions between C and N that affect plant productivity and soil and litter decomposition. Observations from the LIDET data set were compiled for calibration and evaluation of the decomposition submodel within ISAM. For aboveground decomposition, the calibration is accomplished by optimizing parameters related to four processes: the partitioning of leaf litter between metabolic and structural material, the effect of lignin on decomposition, the climate control on decomposition and N mineralization and immobilization. For belowground decomposition, the calibrated processes include the partitioning of root litter between decomposable and resistant material as a function of litter quality, N mineralization and immobilization. The calibrated model successfully captured both the C and N dynamics during decomposition for all major biomes and a wide range of climate conditions. Model results show that net N immobilization and mineralization during litter decomposition are dominantly controlled by initial N concentration of litter and the mass remaining during decomposition. The highest and lowest soil organic N storage are in tundra (1.24 Kg N m^{-2}) and desert soil (0.06 Kg N m^{-2}). The vegetation N storage is highest in tropical forests (0.5 Kg N m^{-2}), and lowest in tundra and desert (<0.03 Kg N m^{-2}). N uptake by vegetation is highest in warm and moist regions, and lowest in cold and dry regions. Higher rates of N leaching are found in tropical regions and subtropical regions where soil moisture is higher. The global patterns of vegetation and soil N, N uptake and N leaching estimated with ISAM are consistent with measurements and previous modeling studies. This gives us confidence that ISAM framework can predict plant N availability and subsequent plant productivity at regional and global scales and furthermore how they can be affected by factors that alter the rate of decomposition, such as increasing atmospheric [CO_2], climate changes, litter quality, soil microbial activity and/or increased N.

Citation: Yang, X., V. Wittig, A. K. Jain, and W. Post (2009), Integration of nitrogen cycle dynamics into the Integrated Science Assessment Model for the study of terrestrial ecosystem responses to global change, *Global Biogeochem. Cycles*, *23*, GB4029, doi:10.1029/2009GB003474.

1. Introduction

[2] Global increases in temperature and atmospheric CO_2 concentrations ([CO_2]) are altering the dynamics of the global carbon (C) cycle [*McGuire et al.*, 2001; *Jain and Yang*, 2005; *Denman et al.*, 2007]. Increasing [CO_2] leads to increased C fixation during photosynthesis, leading to greater inputs of C into vegetation and soils compared to preindustrial [CO_2]. This "CO_2 fertilization effect" has been observed in numerous field experiments [*Koch and Mooney*, 1996; *Curtis*, 1996; *Mooney et al.*, 1999; *Poorter*, 1993; *Norby et al.*, 2005; *DeLucia et al.*, 2005; *Ainsworth and Long*, 2005; *Nowak et al.*, 2004] and has been incorporated into modeling studies explaining the terrestrial C sink [*Friedlingstein et al.*, 1995; *Jain and Yang*, 2005; *McGuire et al.*, 2001; *Post et al.*, 1997]. It has been shown that terrestrial C cycling is sensitive to climate variability and change [*Braswell et al.*, 1997; *Jain and Yang*, 2005; *King et al.*, 1997; *McGuire et al.*, 2001; *Tian et al.*, 1999]. CO_2 fixation by photosynthesis and CO_2 loss by respiration of both plants and soils, are generally increasing with increasing temperature, although soil respiration often increases more rapidly [*Shaver et al.*, 2000]. It has been argued that the net effect of the large increase in respiration

[1]Department of Atmospheric Sciences, University of Illinois at Urbana-Champaign, Urbana, Illinois, USA.
[2]Oak Ridge National Laboratory, Oak Ridge, Tennessee, USA.

0886-6236/09/2009GB003474$12.00

in comparison to small increases in photosynthesis with increasing temperature will result in less C stored in terrestrial ecosystems [*Cao and Woodward*, 1998; *Cramer et al.*, 2001; *Friedlingstein et al.*, 2006; *Berthelot et al.*, 2005; *Ito*, 2005].

[3] However, the terrestrial C cycle is not only directly altered by increasing atmospheric [CO_2], climate change, and anthropogenic N deposition, it also indirectly altered by feedbacks from nitrogen (N) cycle perturbations induced by changes in [CO_2] and climate. This is due to the close coupling of the C and N cycles in the terrestrial biosphere. Plants require N for growth and maintenance of tissues which are eventual inputs into the soil. Soil microbes mineralize the organic N tied up with C in plant tissues during decomposition of litter and soil organic matter (SOM) creating a pool of inorganic N. The inorganic N is then available for plant uptake. Because plant N availability is largely determined by litter and soil decomposition [*Kirschbaum and Paul*, 2002], it therefore follows that any environmental factors that alter the rate of decomposition such as increasing [CO_2], climate changes, litter quality, soil microbial activity and/or increased input of N to the system via N deposition, will alter plant N availability and subsequent plant productivity in regions where nitrogen is a limiting nutrient.

[4] Studies have shown that N cycling is altered under elevated [CO_2] [*Peterson et al.*, 1999; *Norby et al.*, 2001; *Gill et al.*, 2002; *Zak et al.*, 2003; *Hungate et al.*, 2004; *Mosier et al.*, 2002; *Reich et al.*, 2001]. Elevated [CO_2] increases C_3 photosynthesis by competitively inhibiting the oxygenation of Rubisco in favor of the carboxylation reaction [*Long et al.*, 2004]. Enhanced plant growth leads to increased C storage and therefore additional N sequestration in plant biomass and soil organic matter, which leads to the depletion of the soil mineral N pool and therefore could constrain uptake of CO_2 by plants [*Luo et al.*, 2004; *Oren et al.*, 2001; *Finzi et al.*, 2006, 2007; *Reich et al.*, 2006].

[5] Experiments indicate that on short time scales, N use efficiency is increased when the C:N ratio in plant tissue is increased [*Norby et al.*, 1999; *Körner*, 2000]. It has been shown that changes in plant tissue C:N ratio may have a negligible effect on decomposition [*Norby and Cotrufo*, 1998; *Norby et al.*, 2001]. It has also been shown that increased [CO_2] may increase root N uptake [*McGuire et al.*, 1995; *Norby et al.*, 1999]. Experiments also show that mineral N availability in soil could be increased under climate warming through enhanced soil N mineralization, associated with increased decomposition rates[*Rustad et al.*, 2001; *Shaver et al.*, 2000]. The increased mineral N in soil has the potential to enhance the uptake of CO_2 by plants more than the loss of CO_2 from soil respiration [*Rustad et al.*, 2001; *Shaver et al.*, 2000].

[6] Furthermore, the processes that directly or indirectly affect the response of terrestrial C storage to increased [CO_2] operate on a wide range of time scales. For example, observations of increased C fixation and high C:N ratios of litter from elevated [CO_2] experiments can last a few years whereas increased biological N fixation and decreased N loss are long-term mechanisms affecting overall N supply [*Luo et al.*, 2004; *Thornley and Cannell*, 2000]. Thus, the impact of elevated [CO_2] on C and N dynamics derived from short-time-scale experiments i.e., less than 5 years, may not be the same in the long-term i.e., decades to centuries. To evaluate these impacts, modeling studies capable of projecting changes over long time scales are essential.

[7] Several recent studies highlight the importance of N dynamics in regulating the response of terrestrial C cycle to increasing [CO_2] and climate change [*Thornton et al.*, 2007, 2009; *Sokolov et al.*, 2008]. *Thornton et al.* [2007] show that N availability strongly constrains the CO_2 fertilization effect on plant productivity under increasing [CO_2]. *Sokolov et al.* [2008] shows that consideration of N dynamics changes the sign of climate-C cycle feedback. When N dynamics are not considered, *Sokolov et al.* [2008] show that global warming reduces terrestrial C storage, i.e., a positive C-climate feedback. By contrast, when N dynamics are considered, *Sokolov et al.* [2008] found that terrestrial C storage actually increases with moderate increases in surface temperature due to the fertilization of plant growth by increased mineralization of N under climate warming. *Thornton et al.* [2009] also found an overall negative climate–carbon cycle feedback when N cycling is introduced, which is due to the fertilization of plant growth by increased mineralization of N under climate warming.

[8] Despite the close coupling of C and N cycles and the significant impact of N dynamics on terrestrial C storage, few global terrestrial ecosystem models have incorporated the interaction of N dynamics with C cycling and the interactive impact on terrestrial C uptake. The models available to date, e.g., TEM [*McGuire et al.*, 1992], CENTURY [*Schimel et al.*, 1996], Biome-BGC [*Thornton et al.*, 2007] and LPJ [*Xu-Ri and Prentice*, 2008], with the exception of CENTURY, have focused predominantly on plant physiological processes and have simplified the decomposition processes. These models have had limited capacity to simulate N dynamics during litter and SOM decomposition and examine the resultant impacts on terrestrial C cycling. Extensive data from the Long-Term Intersite Decomposition Experiment (LIDET) is now available for the parameterization, calibration and evaluation of a dynamic model of decomposition and N cycling. LIDET was a 10 year reciprocal litter bag study designed to study the effects of substrate quality and global macroclimate on litter decomposition and N availability via immobilization and mineralization [*LIDET*, 1995; *Parton et al.*, 2007]. LIDET provides an ideal data set for the development and testing of the factors governing decomposition in a broad range of ecosystems with varying climatic regimes.

[9] The Integrated Science Assessment Model (ISAM) was originally developed as a tool to project the likely impacts of future changes in [CO_2] on terrestrial ecosystems as a result of fossil fuel burning, land use and land cover change and forest fires [*Jain et al.*, 1996; *Jain and Yang*, 2005; *Tao and Jain*, 2005; *Jain et al.*, 2006] and has been used in IPCC assessments to assess the future climate change scenarios [*Schimel et al.*, 1996; *Prentice et al.*, 2001]. The objective of the current study is to extend upon previous modeling work with ISAM detailing the C

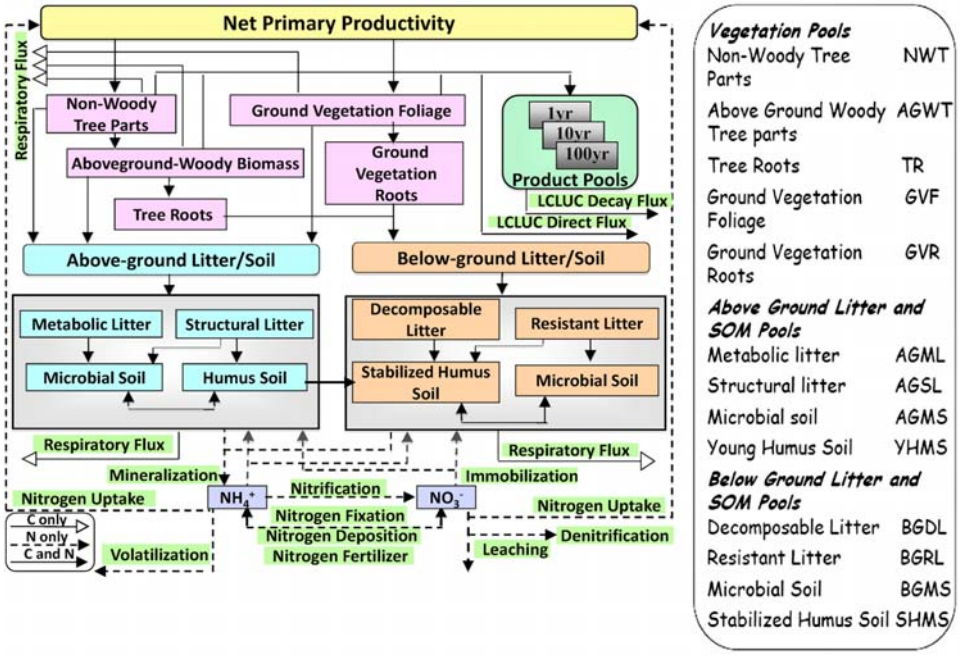

Figure 1. Schematic diagram of all reservoirs and flows in the ISAM coupled carbon–nitrogen cycle model. The side panel shows the abbreviations of different pools used in the text.

dynamics of the terrestrial biosphere [*Jain and Yang*, 2005; *Jain et al.*, 1995; *Jain et al.*, 1996] and couple this to the N cycle. The objective is achieved here through the development of a comprehensive model of terrestrial N dynamics and the coupling of this model with the geographically explicit terrestrial C cycle component of ISAM [*Jain and Yang*, 2005]. Specifically, this study is designed to (1) describe the structure and formulations of ISAM as modified to include a fully coupled N cycle, (2) calibrate and evaluate the newly defined N cycle processes (N mineralization and immobilization) via simulated estimates of litter and soil decomposition across a range of biomes using LIDET data, and (3) estimate and compare global mean pools and fluxes of N between vegetation and soils with measurements and other model studies.

[10] In a companion paper [*Jain et al.*, 2009], the model described here is used to investigate how the N cycle influences on the terrestrial C cycle in response to changes in [CO_2], climate, N deposition and land use during the 20th century.

2. Integrated Science Assessment Model Description

[11] The Integrated Science Assessment Model (ISAM) is composed of fully coupled atmospheric, oceanic and terrestrial biosphere reservoirs with the capacity to project the interactive effects of changes occurring within reservoirs, i.e., atmospheric chemistry, ocean C cycling and/or terrestrial productivity, in the context of global changes in climate, greenhouse gas emissions, N deposition, land cover and land use [*Jain and Yang*, 2005; *Tao and Jain*, 2005; *Cao and Jain*, 2005, 2008]. The terrestrial C cycle model in ISAM simulates C fluxes to and from different compartments of the terrestrial biosphere within grid cells with 0.5° by 0.5° spatial resolution [*Jain and Yang*, 2005]. Each grid cell is completely occupied by at least one of the twelve land coverage classifications defined in Table S1.[1] Within each grid cell, ISAM simulates evapotranspiration, photosynthesis, autotrophic respiration, plant C allocation, litter production, and soil organic C decomposition. A complete description of the dynamics of the terrestrial C cycle model in ISAM is given by *Jain and Yang* [2005].

2.1. Extended ISAM Structure

[12] ISAM as described by *Jain and Yang* [2005] was extended to enable the explicit study of C and N dynamics, specifically accounting for the effect of mineral N availability on net primary productivity (NPP), through the development of a process-based representation of the complete N cycle. The N cycle model includes formulations describing N deposition, N fixation, N mineralization, N immobilization, nitrification, denitrification, and leaching (Figure 1). In order to study the interactive effects of C and N dynamics, comprehensive litter and SOM decomposition modules were developed. The factors integrated into ISAM that interact with the N cycle to impact litter and SOM decomposition include plant N uptake, litter quality, (i.e., C:N ratio), [N] and [lignin], climate, (i.e., temperature and precipitation), N addition, (i.e., deposition and input from agricultural fertilizer) and [CO_2].

[13] The original C cycle model in ISAM is composed of six compartments: ground vegetation, nonwoody tree parts, woody tree parts, detritus, active soil and resistant soil organic C. In the current extended version of ISAM, the

[1] Auxiliary materials are available in the HTML. doi:10.1029/2009GB003474.

ground vegetation (GV) pool is partitioned into ground vegetation foliage (GVF) and ground vegetation root (GVR); nonwoody tree parts (NWT) are unchanged; woody tree parts (WT) are partitioned into aboveground woody parts (AGWT), and tree roots (TR) (Figure 1). Additional, extensive modifications were made to the litter and SOM pools which now are composed of 8 reservoirs: (1) aboveground metabolic litter (AGML), (2) aboveground structural litter (AGSL), (3) belowground decomposable plant litter (BGDL), (4) belowground resistant plant litter (BGRL), (5) aboveground microbial soil (AGMS), (6) young humus soil (YHMS), (7) belowground microbial soil (BGMS), and (8) stabilized humus soil (SHMS). In addition, two inorganic N reservoirs, ammonium N and nitrate N, are added (Figure 1).

[14] ISAM also considers how C and N dynamics are influenced by land cover and land use change (LCLUC) activities [*Jain and Yang*, 2005]. When natural vegetation changes due to LCLUC activities in a grid cell, a specified amount of vegetation biomass is transferred to litter reservoirs representing slash left on the ground. There are two possibilities considered for the remaining plant material. The remaining plant material could be burned due on LCLUC activities such as clearing the land for agriculture. In this scenario, the C and N previously contained in the burned plant material are released directly to the atmospheric pool as a LCLUC Direct Flux (Figure 1). Alternatively, the C and N are transferred to wood and/or fuel product reservoirs comprising Product Pools (Figure 1). Carbon and N stored in the Product Pools are released to the atmosphere via LCLUC Decay Flux (Figure 1) at rates dependent on usage [*Jain and Yang*, 2005].

[15] The equations are as follows, and variables and parameters are given in Table 1.

For the effect of nitrogen availability on NPP,

$$f_{\mathrm{NPP}}(\mathrm{N}) = a + b \times e^{-c \times x} \tag{1}$$

For the change of N content of above and belowground litter and soil organic pools (i),

$$\frac{d\mathrm{N}_i}{dt} = \frac{d\mathrm{C}_i}{dt} / (\mathrm{C/N})_i \tag{2}$$

For the N mineralized or immobilized amount due to decomposition of i pool to product pool j,

$$\mathrm{N}_M = \left(\frac{d\mathrm{C}_i}{dt}\right) / (\mathrm{C/N})_i - \left(\frac{d\mathrm{C}_i}{dt}\right) \times E_i / (\mathrm{C/N})_j \tag{3}$$

For the amount of N nitrified from ammonium N to nitrate N,

$$\mathrm{N}_{\mathrm{nitri}} = \mathrm{N}_{\mathrm{NH4}} \left(1 - e^{-r \times fB(T) \times fB(W)}\right) \tag{4}$$

For the amount of N denitrified,

$$\mathrm{N}_{\mathrm{den}} = \mathrm{N}_{\mathrm{NO3}} \times (\mathrm{CO}_2)_l \times D \times P \tag{5}$$

For the N nitrate leaching amount,

$$\mathrm{N}_{\mathrm{leach}} = \mathrm{N}_{\mathrm{NO3}} \times \frac{R}{\mathrm{FC}} \tag{6}$$

For the change in carbon content (C_i) of aboveground soil and litter pools,

$$\frac{d\mathrm{C}_i}{dt} = -K_i \times \mathrm{C}_i \times \mathrm{DEFAC}[fA(T), fA(W)] \times f(\mathrm{Lig}) \times f(\mathrm{N}) \tag{7a}$$

For the change in carbon content (C_i) of belowground soil and litter pools,

$$\frac{d\mathrm{C}_i}{dt} = -K_i \times \mathrm{C}_i \times fB(T) \times fB(W) \times f(\mathrm{N}) \times f(P) \tag{7b}$$

For the climate factor,

$$\mathrm{DEFAC} = fA(T) \times fA(W) \tag{8a}$$

For the temperature term,

$$fA(T) = 0.08 \times \exp(0.095 \times T_{\mathrm{soil}}) \tag{8b}$$

For the soil water term,

$$fA(W) = \frac{1.0}{1.0 + 30 \times \exp(-8.5 \times w_{\mathrm{rat}})} \tag{8c}$$

For the lignin concentration factor,

$$\begin{aligned} f(\mathrm{Lig}) &= \exp(-\alpha \times \mathrm{L}_s) (\text{for AGSL pool}) \\ f(\mathrm{Lig}) &= 1 (\text{for other pools}) \end{aligned} \tag{9}$$

For the scalar modifier representing the effects of soil temperature on decomposition rates of soil reservoirs,

$$fB(T) = \frac{47.9}{1 + \exp(106/(T + 18.3))} \tag{10}$$

For the balance between potential N supply and demand for litter and soil decomposition,

$$\beta = \mathrm{N}_{\mathrm{NH4}} + \mathrm{N}_{\mathrm{NO3}} + \sum_i \frac{d\mathrm{N}_i}{dt} - \sum_i \frac{d\mathrm{C}_i}{dt} \times E_i / (\mathrm{C/N})_j \tag{11a}$$

where i stands for decomposing pool, and j stands for humus or microbial pool.

For the nitrogen status of litter and soil organic matter pools (i) during decomposition,

$$\mathrm{N}_{\mathrm{stat}(i)} = \frac{d\mathrm{N}_i}{dt} - \frac{d\mathrm{C}_i}{dt} \times E_i / (\mathrm{C/N})_j \tag{11b}$$

For the nitrogen available for the decomposition of N limited pools,

$$\mathrm{N}_{\mathrm{sup}} = \mathrm{N}_{\mathrm{NO3}} + \mathrm{N}_{\mathrm{NH4}} + \sum\nolimits_i \mathrm{N}_{\mathrm{stat}(i)} \text{ if } \mathrm{N}_{\mathrm{stat}(i)} >= 0 \tag{11c}$$

Table 1. Variables and Parameters That Appear in Model Equations

Symbol	Definition	Value	Source
x	Ratio of N supply and demand for plants		
a, b, and c	Parameters used in equation (1)	$a/b/c$	*McGuire et al.* [1992]
	Tropical evergreen	1.00/0.00/0.00	*McGuire et al.* [1992]
	Tropical deciduous	1.00/0.00/0.00	*McGuire et al.* [1992]
	Temperate evergreen	1.25/−1.25/1.60	*McGuire et al.* [1992]
	Temperate deciduous	1.25/−1.25/1.60	*McGuire et al.* [1992]
	Boreal forest	1.50/−1.50/1.10	*McGuire et al.* [1992]
	Savanna	1.60/−1.60/0.98	*McGuire et al.* [1992]
	Grassland	1.50/−1.50/1.10	*McGuire et al.* [1992]
	Shrubland	1.56/−1.56/1.00	*McGuire et al.* [1992]
	Tundra	1.87/−1.87/0.76	*McGuire et al.* [1992]
	Desert	1.09/−1.09/2.45	*McGuire et al.* [1992]
	Polar desert	2.00/−2.00/0.69	*McGuire et al.* [1992]
	Cropland	1.00/−1.00/0.00	*McGuire et al.* [1992]
	Pastureland	1.00/−1.00/0.00	*McGuire et al.* [1992]
$(C:N)_{ABSL}$	C:N Ratio of ABSL pool	150	*Parton et al.* [1987]
$(C:N)_{AGML}$	C:N Ratio of AGML pool	Varies	see section 2.2.2
$(C:N)_{AGMS}$	C:N Ratio of AGMS pool	8–30	see section 2.2.2
$(C:N)_{YHMS}$	C:N Ratio of AGMS pool	Varies	see section 2.2.2
$(C:N)_{BGDL}$	C:N Ratio of AGMS pool	Varies	see section 2.2.2
$(C:N)_{BGRL}$	C:N Ratio of AGMS pool	Varies	see section 2.2.2
$(C:N)_{BGMS}$	C:N Ratio of BGMS pool	8	*Bradbury et al.* [1993] and *Bauhus and Khanna* [1999]
$(C:N)_{SHMS}$	C:N Ratio of SHMS pool	Varies	see section 2.2.2
E_i	microbial efficiency of the ith pool		
	AGML, AGSL, AGMS, YHMS	0.45, 0.30, 0.60, 0.55	*Moorhead et al.* [1999]
	BGGL, BGRL, BGMS, SHMS	$(1 - F_{CO2})$, function of soil clay fraction	see equation (18)
N_{NH4}	amount of ammonium N in soil		
r	rate constant of nitrification	0.16 week^{-1}	*Bradbury et al.* [1993]
N_{NO3}	amount of nitrate N in soil		
$(CO_2)_l$	C lost due to respiration during the decomposition of SOM (acting as a surrogate for biological activity)		
D	denitrification factor	50 (kg C)$^{-1}$ m^{-2}	*Bradbury et al.* [1993]
FC	field capacity		
P	ratio of soil moisture and FC		
R	Excess water, which moves downward out of the soil layer after the soil has reached its field capacity (FC)		
K_i	decomposition rate of the ith reservoir (yr^{-1})		
	AGML, AGSL, AGMS, YHMS	4.5, 18.5, 7.3, 2.0	*Moorhead et al.* [1999]
	BGDL, BGRL, BGMS, SHMS	10.0, 0.3, 0.66, 0.02	*Jenkinson* [1990]
T_{soil}	soil temperature		
w_{rat}	ratio of available water (precipitation plus stored soil water) and potential evapotranspiration		
L_s	lignin concentration		
α	empirical factor that describes the extent to which decomposition is slowed down as the lignin concentration increases.	1.5	calibrated based on LIDET data for litter mass loss
$f(P)$	scalar modifiers representing the effects of plant protection on decomposition rates of soil reservoirs	0.6	*Jain and Yang* [2005]
T	monthly temperature (°C).		see section 2.3.2
$fB(W)$	scalar modifiers representing the effects of soil moisture deficit on decomposition rates of soil reservoirs	0.2–1	see section 2.3.2
N_{max}	maximum rate of nitrogen uptake by vegetation		*Raich et al.* [1991][a]
K_{nl}	concentration of N_{av} at which N uptake proceeds at one-half its maximum rate	1.0 g N m^{-2}	*Raich et al.* [1991]
M	soil water		
S_{AGMS}	fraction of decomposed AGMS that is stabilized and transferred to YHMS pool	0.1	*Corbeels et al.* [2005]
S_{YHMS}	fraction of decomposed YHMS that is stabilized and transferred to SHMS pool	0.1	*Corbeels et al.* [2005]

[a]For few grid points the value of N_{max} is adjusted in the steady state run to get the balance between the annual nitrogen uptake and nitrogen litter production.

For the nitrogen needed to support decomposition of N limited pools,

$$N_{ned} = \sum\nolimits_i N_{stat(i)} \text{ if } N_{stat(i)} < 0 \quad (11d)$$

For the nitrogen limitation factor for decomposition of litter and soil organic matter pools,

$$f(N) = \begin{cases} \frac{N_{sup}}{N_{ned}} & \text{if } N_{stat(i)} < 0 \\ 1 & \text{if } N_{stat(i)} >= 0 \end{cases} \quad (11e)$$

For the N uptake by vegetation,

$$N_{uptake} = \frac{N_{max} \times K_S \times (N_{NH4} + N_{NO3})}{K_{nl} + K_S \times (N_{NH4} + N_{NO3})} \times e^{0.0693 \times T_{soil}} \times f_{root} \quad (12a)$$

For the N uptake by vegetation from NH_4 pool in soil,

$$N_{uptake,NH4} = \frac{N_{NH4}}{N_{NO3} + N_{NH4}} \times N_{uptake} \quad (12b)$$

For the N uptake by vegetation from NO_3 pool in soil,

$$N_{uptake,NO3} = \frac{N_{NO3}}{N_{NO3} + N_{NH4}} \times N_{uptake} \quad (12c)$$

For the parameter accounting for relative difference in the conductance of the soil to nitrogen diffusion,

$$K_S = 0.90(M/FC)^3 + 0.10 \quad (13)$$

For the factor that weights plant nitrogen uptake based on root C,

$$f_{root} = 1.0 - 0.8e^{-root\_C \times 0.015 \times 2.5} \cdot \left(root\ C \times 0.015 \times 2.5 < 33\ g\,C\,m^{-2}\right)$$
$$f_{root} = 1\left(root\ C \times 0.015 \times 2.5 \geq 33\,g\,C\,m^{-2}\right) \quad (14)$$

For the dead foliage litter for AGML pool,

$$f_{ml} = 0.85 - 0.018 \times L_s/N \quad (15a)$$

For the dead foliage litter for AGSL pool,

$$f_{sl} = 1 - f_{ml} \quad (15b)$$

For the fraction of C contents in ith pool lost as CO_2,

$$1 - E_i, \quad (16a)$$

For the fraction of C contents in ith pool (i.e., AGMS and YHMS) that is stabilized and humified,

$$E_i \times S_{AGMS} \text{ or } E_i \times S_{YHMS} \quad (16b)$$

For the root litter for BGDL pool,

$$f_d = 0.74 - 0.015 \times L_s/N \quad (17a)$$

For the root litter for BGRL pool,

$$f_r = 1 - f_d \quad (17b)$$

For the C transferred to atmosphere from BGDL and BGRL pools,

$$F_{CO2} = y/(1+y)$$
$$y = 1.67 \times [1.85 + 1.60 \times \exp(-0.786 \times \text{soil clay fraction in \%})] \quad (18)$$

[16] The model operates on two time steps. The vegetation submodel operates on yearly time step, e.g., NPP, litter production and N demand by vegetation are calculated annually. Annual litter production is equally distributed into each week of a year to provide the weekly litter input. Litter and soil decomposition, N immobilization, N mineralization, N uptake, denitrification, nitrification, and N leaching are calculated weekly. The N uptake for each week is summed to calculate annual N uptake. This value is then compared with annual N demand to determine the effect of N availability on NPP as described by equation (1).

2.2. Nitrogen Dynamics of Different Reservoirs

2.2.1. Nitrogen Dynamics of Vegetation Reservoirs

[17] The effect of mineral N availability on NPP is dynamically determined by comparing plant N supply and demand. The initial [N] in each vegetation reservoir is calculated based on its C:N ratio as defined in Table S1, based on the assumption that 50% of vegetation biomass is C [*Smith et al.*, 2003]. At each yearly time step, total N demand is a function of initial [N] of plant tissues and new growth. N supply is the sum of annual N retranslocation from foliage prior to litter fall and annual N uptake by plants. N retranslocation determines the rate of N movement from the vegetation pools prior to litterfall for plant to use in next year. It is assumed that there is no retranslocation of N in woody and root reservoirs. The retranslocation rate for GVF is assumed to be 50% for all biome types [*White et al.*, 2000], whereas the retranslocation rate for the NWT reservoir is prescribed for each forest ecosystem (Table S1). Plant N uptake is dependent on mineral N availability, temperature, soil moisture, and root mass; and is discussed in section 2.4. The ratio of N supply to N demand is used to estimate the effect of N availability on NPP following equation (1). When the calculated N demand is greater than N supply, NPP is scaled back to the level that N supply can support. For example, under conditions of N limitation, photosynthesis is down regulated, therefore reducing NPP. On the other hand, if N demand is less than supply, plant production is enhanced and NPP is increased accordingly until reaching the N saturation point [*McGuire et al.*, 1992].

[18] N allocation in vegetation reservoirs is calculated annually and after litter N production (section 2.4). The total amount of N available for allocation in vegetation is the sum

of plant N supply and all vegetation N. N allocation is calculated in such a way that relative C:N ratios among the vegetation reservoirs are fixed, while the C:N ratio of any one vegetation reservoir is allowed to vary as a function of N uptake and loss [*Friend et al.*, 1997].

2.2.2. Nitrogen Dynamics of Aboveground and Belowground Litter and Soil Organic Matter Reservoirs

[19] Changes in the N content of aboveground and belowground litter and SOM reservoirs follow changes in C content (see section 2.3.2). The [N] of litter and SOM is equal to the product of changes in C and C:N ratio of each reservoir (equation (2)). We assume the C:N ratio of AGSL reservoir to be fixed at 150 [*Parton et al.*, 1987], whereas the C:N ratio of AGML reservoir varies with the overall [N] of aboveground litter. The C:N ratio for microbial soil varies greatly and studies have given different ranges for its value. For example, *Moorhead et al.* [1999] assumes that C:N ratio of microbial soil varies between 12 and 22, while *Corbeels et al.* [2005] indicates it ranges between 5 and 30. We use LIDET data to calibrate the C:N ratio of AGMS pool increasing between 8 and 30 as the [N] of incoming litter decreases from 2% to 0.1%. The C:N ratio for YHMS reservoir is assumed to be C:N ratio of AGMS reservoir plus 6, which is determined by fitting the model to observed rates of nitrogen mineralization during litter decomposition in other experiments [*Moorhead et al.*, 1999], and is also evaluated with data from LIDET in this study.

[20] The C:N ratios of BGDL and BGRL are allowed to vary, but they maintain a constant proportionality between them. Here we assume that the C:N ratio of BGRL is three times the C:N ratio of BGDL reservoir. This relationship is determined by fitting the model to measured [N] data based on LIDET experiments. The C:N ratio of BGMS reservoir is assumed to be 8, which is the mean value determined in 119 temperate, tropical, and boreal forest soils [*Bauhus and Khanna*, 1999]. The C:N ratio for SHMS reservoir is allowed to vary depending on the overall [N] of the material transferred into SHMS reservoir.

[21] During the decomposition of both aboveground and belowground litter and SOM pools, part of C is respired. The remaining C cycles between litter and SOM pools as shown in Figure 1. Both immobilization and mineralization of N can occur during decomposition depending on the C:N ratio of the litter and SOM pools and the microbial efficiency (equation (3)). If the transferred amount of C requires less N to maintain the specified C:N ratio of humus and microbial pool, N will be mineralized ($N_M > 0$ in equation (3)). In contrast, if the transferred amount of C requires additional N to maintain the specified C:N ratio, immobilization of inorganic N from both soil mineral reservoirs, i.e., ammonium and nitrate, will occur ($N_M < 0$ in equation (3)). If there is not enough mineral N to meet immobilization demand, decomposition rate is reduced as discussed in section 2.3.2.

2.2.3. Nitrogen Dynamics of Soil Inorganic Nitrogen Reservoirs

2.2.3.1. Biological N Fixation and N Deposition

[22] A regression analysis of literature-based estimates of N fixation on ecosystem evapotranspiration (ET) [*Cleveland et al.*, 1999] demonstrates that there are significant relationships between ET and N fixation: ET accounted for >60% of the variability in the whole range of estimates of N fixation. This suggests that at the ecosystem level, ET is a reasonable predictor of N fixation. In this study, we incorporated the empirical function developed by *Schimel et al.* [1996] to estimate BNF based on ET. We modified the parameters in the function in such a way as to the estimated BNF for each biome type in accordance with that given by *Cleveland et al.* [1999]. Another input for inorganic N in soil is atmospheric wet and dry deposition. In this study, we use the deposition data from 1765 provided by *Galloway et al.* [2004].

2.2.3.2. Nitrification and Denitrification

[23] During nitrification, ammonium N is nitrified to nitrate N. This is modeled at each time step according to equation (4) [*Bradbury et al.*, 1993]. Denitrification transforms nitrate N into gaseous N (NO, N_2O, N_2), which is then released to the atmospheric reservoir according to equation (5) [*Bradbury et al.*, 1993]. Since denitrification in the soil is strongly related to CO_2 production [*Bradbury et al.*, 1993], the amount of N denitrified in each time step is proportional to the amount of CO_2 produced from SOM decomposition (equation (6)). Further, we assume that the maximum rate of denitrification occurs when the soil is at the maximum water holding capacity. If the soil water is unsaturated, the denitrification rate decreases in proportion to the ratio of soil moisture and field capacity (P).

2.2.3.3. Nitrate Leaching and Volatilization

[24] It is assumed that nitrate N is infinitely soluble in water and moves downward out of the soil layer at the same rate as the water in which it is dissolved. The amount the nitrate N leaching out of the soil is determined by the soil nitrate N pool, field capacity of the soil (FC), and percolation (R) according to equation (6). Percolation occurs when the water entering the soil layer is more than that needed to saturate it. The soil water budget model by *Pastor and Post* [1985] as implemented by [*Jain and Yang*, 2005] was used to calculate soil water content and percolation. NH_4^+ N can be lost by volatilization after the application of N fertilizers and is modeled using the formulations of *Bradbury et al.* [1993]. The N volatilization flux in this study is zero; because N fertilizers input are not considered in this study.

2.3. Carbon Dynamics of Different Reservoirs

2.3.1. Carbon Dynamics of Vegetation Reservoirs

[25] Net primary production (kg C m^{-2} yr^{-1}) for the GVF, NWT and AGWT pools varies with vegetation C according to empirical plant growth equations [*Jain et al.*, 1996; *Kheshgi et al.*, 1996; *King et al.*, 1995]. The photosynthetically active vegetation carbon reservoirs are characterized by their turnover times and the rate of exchange between them. The values of these parameters for each of our model's land cover types are calculated from the specified initial values of fraction of tree and ground vegetation carbon (kg C m^{-2} yr^{-1}) as described in detailed by *Jain and Yang* [2005]. The modeled NPP is consistent with other studies [*Prentice et al.*, 2001; *Cramer et al.*, 1999] as noted by *Jain and Yang* [2005]. The GVF and NWT reservoirs fix C by photosynthesis, while the remaining AGWT, TR, and GVR release C by respiration. Net

photosynthesis of ground vegetation is partitioned equally into GVF and GVR [*Post et al.*, 1997; *Potter and Klooster*, 1997; *Friedlingstein et al.*, 1999]. The C in tree reservoirs is allocated between NWT, AGWT, and TR. The allocation of C between NWT and AGWT were derived by *Jain and Yang* [2005]. The allocation of C between AGWT and TR is determined based on the lifetime and mass fraction of tree roots for each land cover type [*King et al.*, 1997].

2.3.2. Carbon Dynamics of Aboveground and Belowground Litter and Soil Reservoirs

[26] The C dynamics for aboveground litter (AGML and AGSL) and soil (AGMS and YHMS) pools are based on the CENTURY model [*Parton et al.*, 1987, 1994; *Moorhead et al.*, 1999] taking into account both environmental and biological drivers of decomposition, namely temperature, soil moisture, and quality of aboveground litter. The belowground litter, i.e., dead roots and soil organic C dynamics, are estimated based on the Rothamsted soil turnover model (RothC) [*Jenkinson*, 1990]. This model has been successfully applied to estimate soil organic matter turnover for agriculture and forest biomes [*King et al.*, 1997; *Jain and Yang*, 2005; *Smith et al.*, 1997; *Paul and Polglase*, 2004].

[27] The changes in C content of aboveground and belowground soil and litter pools are calculated according to equations (7a) and (7b). The decomposition rates (K_i) of aboveground reservoirs are modified by a climate factor (DEFAC) (equation (8a)), a temperature term $fA(T)$ (equation (8b)), a soil water term $fA(W)$ (equation (8c)) [*Parton et al.*, 1994] and a [lignin] factor $f(Lig)$ [*Parton et al.*, 1987]. The value of $f(Lig)$ for the AGSL pool is calculated by equation (9). In equation (7b), $fB(T)$, $fB(W)$, $f(P)$ are the scalar modifiers representing the effects of soil temperature, soil moisture deficit, and plant protection on decomposition rates of soil reservoirs [*Jenkinson*, 1990]. The $fB(T)$ is calculated by equation (10). The $fB(W)$ varies between 0.2 and 1.0. It is 1.0 for deficits ranging from field capacity i.e., millimeter water held at -33 kPa tension, to a water pressure of -100 kPa. The $fB(W)$ decreases linearly from 1.0 at -100 kPa to 0.2 at a soil moisture deficit with a tension of -1500 kPa, i.e., plant wilting point.

[28] The litter and soil decomposition rates are further reduced due to the limitation of N availability, as represented by $f(\mathrm{N})$ in equations (7a) and (7b). In this study $f(\mathrm{N})$ for each litter and soil pool is determined according to formulation of *Moorhead and Reynolds* [1991]. First, the potential changes in C content of all litter and soil organic matter pools are estimated using equations (7a) and (7b) by assuming there is no N limitation (e.g., $f(\mathrm{N}) = 1$ for all pools). The potential change of N content for each pool is then estimated using equation (2). The balance between the potential N availability and demand for all pools determines if the decomposition of litter and soil is N limited or not (equation (11a)) [*Moorhead and Reynolds*, 1991]. If potential N availability is greater than the demand ($\beta > 0$ in equation (11a)), decomposition is not N limited ($f(\mathrm{N}) = 1$ for all litter and soil pools). On the other hand, if the N availability is less than demand ($\beta < 0$ in equation (11a)), decomposition is N limited and the N status of each pool is estimated with equation (11b). The extent to which decomposition of each pool is limited by N is estimated according to equations (11c), (11d), and (11e) [*Moorhead and Reynolds*, 1991].

2.4. Coupling of Carbon and Nitrogen Cycles

[29] C and N in vegetation and soil are linked through litter fall, decomposition, N mineralization and N uptake by vegetation. When litter composed of C and N decomposes, C is released as CO_2 and N is mineralized and becomes available for vegetation uptake.

[30] Litter is produced from turnover of vegetation at rates that vary with temperature [*Jain et al.*, 1996; *Jain and Yang*, 2005]. Three types of litter are considered in this study: leaf litter, wood litter and root litter. The GVF and NWT reservoirs supply foliage litter, AGWT supplies wood litter and GVR and TR are the sources of root litter. It is assumed that the C in litter for a vegetation pool is the ratio of C mass and turnover time. The N in litter is calculated in the same way as litter C production, except that N retranslocation is considered for foliage litter allowing a fraction of foliage N retranslocation into the plants prior to litter loss (section 2.2.1). Plants take up N from both ammonium N and nitrate N pools. The amount of N taken up by plants at each time step is estimated by utilizing Michaelis-Menten kinetics [*Raich et al.*, 1991] (equations (12a), (12b), and (12c)).

2.5. Distribution of Aboveground and Belowground Litter

[31] Aboveground litter includes dead foliage and dead wood. Dead foliage is partitioned into AGML and AGSL pools based on lignin (L) and N ratio (L/N) (see equations (15a) and (15b)) [*Parton et al.*, 1987; *Kirschbaum and Paul*, 2002]. It is assumed that all of the lignin from the incoming foliage litter flows into the AGSL [*Parton et al.*, 1987]. Accordingly, lignin from wood litter is entered into AGSL [*Kirschbaum and Paul*, 2002; *Corbeels et al.*, 2005]. Litter in AGML and AGSL reservoirs decompose into AGMS and YHMS at rates according to equation (7a). A fraction of C contents (equation (16a)) is lost as CO_2 to the atmosphere. It is assumed that the [lignin] of the AGSL pool is only transferred into the YHMS pool based on experimental findings that suggest lignin is largely found in humus material [*Stott et al.*, 1983]. When microbial biomass in AGBS is decomposed, a part of the C is lost due to microbial respiration (equation (16a)). Another part of the decomposed microbial biomass (S_{AGMS}), which represents synthesis of hydrolysable humified microbial products [*Azam et al.*, 1985], is transferred to YHMS pool (equation (16b)). The rest reenters AGBS due to microbial succession. When humus litter in YHMS pool is decomposed, a fraction of C is lost as CO_2 into the atmosphere (equation (16a)). A part of the C (S_{YHMS}) is transferred to the long-lived SHMS pool (equation (16b)), representing the synthesis of stabilized humified microbial products [*Corbeels et al.*, 2005], and the remaining C is transferred to the AGMS.

[32] The incoming belowground root litter material directly enters the BGDL and BGRL pools. The formulations for the amount of C that enters each pool is calibrated with LIDET root litter data and are given by equations (17a) and (17b). When the organic material in these reservoirs is decomposed, a part of C is lost to the atmosphere, and the

Table 2. Sites Chosen in This Study for Calibrations and Validation of ISAM Model and MAP and MAT at Those Sites[a]

Biome	Site (Code)	Location	MAP (mm)	MAT (°C)
Tropical forest	Luquillo (LUQ)	Puerto Rico	3500	22.1
	Monteverde Cloud Forest Reserve(MTV)	Costa Rica	2685	17.6
Temperate forest	Coweeta Hydrological (CWT)	North Carolina	1847	12.5
	H.J Andrews Experimental Forest (AND)	Oregon	2291	9.3
Boreal forest	Bonanza Creek (BNZ)	Alaska	260	−3.6
	Juneau (JUN)	Alaska	1367	4.4
Tundra	Arctic Tundra (ARC)	Alaska	284	−7.0
	Niwot Ridge/Green Lakes (NWT)	Colorado	931	−3.7
Grassland	Konza Prairie (KNZ)	Kansas	835	12.7
	Jornada (JRN)	New Mexico	233	14.6

[a]MAP, Mean Annual Precipitation; MAT, Mean Annual Temperature.

rest enters into BGBS and SHMS reservoirs. The fraction of CO_2 (F_{CO2}) released to the atmosphere is calculated by equation (18) [*Jenkinson*, 1990]. The ratio of C entering BGBS and SHMS pools is assumed constant of 1.67 for all soils [*Jenkinson*, 1990]. When BGBS and SHMS are decomposed, CO_2 is released to the atmosphere, and the material (microbial and humus) in these pools are regenerated according to the same ratio as that of decomposed BGDL and BGRL.

3. Long-Term Intersite Decomposition Experiment Data for ISAM Calibration and Evaluation

3.1. LIDET Data

[33] Data used for the calibration and evaluation of models of C and N content in litter and soil pools were compiled from the Long-Term Intersite Decomposition Experiment (LIDET). LIDET was a reciprocal litter bag study initiated in 1989 to study the effects of substrate quality and global macroclimate on decomposition, nutrient immobilization and mineralization over a 10 year period [*LIDET*, 1995; *Parton et al.*, 2007]. The LIDET study provides litter data across several biomes in North and Central America for mass loss, litter quantity, [N], initial [lignin], and temperature and precipitation for long-term, i.e., 10 year, litter decomposition [*Gholz et al.*, 2000; *Moorhead et al.*, 1999]. The LIDET data employed here was first used to calibrate decomposition properties of contrasting litter types. In this way, it is possible for ISAM to simulate decomposition rates of litter types that fall on or between the contrasting litter extremes. Additional LIDET data was next used to evaluate the calibration.

[34] In total there are 28 sites involved in the LIDET. Ten LIDET sites representing five biomes directly comparable to the biomes defined in ISAM were selected for calibration and evaluation purposes in this study, with each biome represented by two replicate sites (Table 2). The sites chosen here met the following criteria: (1) minimum within-site variation and (2) the most extensive data available as compared to other sites in LIDET data set. The decomposition data of a core set of five leaf-litter and three root-litter types decomposed at each of the ten selected sites were used in this study for calibration and evaluation (Table 3). This core set of litter types encompass a wide range of litter qualities, i.e., C:N ratios and N: Lignin ratios (Table 3) and therefore decomposition rates. Specifically, the decomposition data from two leaf litter types with contrasting C:N and N:Lignin, (*Drypetes glauca* and *Triticum aestivum*), were used for the calibration of aboveground litter pools. *Drypetes glauca* has 1.98% N and 10.9% Lignin and C:N of 25 and N:Lignin of 0.18. *Triticum aestivum* has 0.38% N and 16.2% Lignin and C:N of 138 and N:Lignin of 0.023 (Table 3). Next, leaf litter data from selected LIDET sites with *Pinus resinosa*, *Acer saccharum*, *Quercus prinus* were used to evaluate the aboveground litter decomposition properties (Table 3). Similarly, decomposition data from the two core root litters with contrasting properties, *Pinus elliottii*, *Drypetes glauca*, were used for the calibration of belowground decomposition. *Andropogon gerardii* root litter data was used for evaluation of belowground decomposition at all chosen sites (Table 3).

3.2. ISAM Calibration

[35] Calibration of both aboveground and belowground litter decomposition is performed in two steps. First, the C dynamics of parameters controlling litter decomposition are calibrated. Next, the parameters controlling N immobilization and mineralization are calibrated. Calibration is performed by minimizing the total sum of the squares of the difference between predicted and observed C or N of decaying litter remaining for all chosen species and sites. This is realized through automatic optimization using the FFSQP (FORTRAN implementation of the Feasible Sequential Quadratic Programming) numerical optimization scheme [*Zhou et al.*, 1997]. Under certain conditions an automatic optimization scheme is not able to give parameter values with results close to observations, particularly when there is a large year-to-year variation in the observational data. In such cases, trial and error is used to find parameters that achieve the least absolute difference between predicted and observed values.

[36] For aboveground litter decomposition, the calibration is accomplished by optimizing the parameters relating to

Table 3. Initial Quality of Core Litters Used to Calibrate and Validate the Model

Litter Type	Specie (Acronym)	Lignin (%)	N (%)	Lignin/N
	Calibration			
Leaf litter	*Triticum aestivum* (TRAE)	16.2	0.38	42.63
	Drypetes glauca (DRGL)	10.9	1.98	5.5
Root litter	*Pinus elliottii* (PIEL)	34.9	0.82	42.5
	Drypetes glauca (DRGL)	16.1	0.76	21.18
	Validation			
Leaf litter	*Pinus resinosa* (PIRE)	19.2	0.58	33
	Acer saccharum (ACSA)	15.9	0.80	19
	Quercus prinus (QUPR)	23.5	1.02	23
Root litter	*Andropogon gerardii* (ANGE)	10.5	0.63	16.67

Table 4. Major Processes and Parameters Calibrated

Calibrated Process	Equations	Parameters	Parameter Values: Original	Parameter Values: Calibrated
	Aboveground			
Partitioning of litter between AGML and AGSL	$f_{ml} = a - b \times L/N$	a, b	0.85, 0.018	0.85,0.018
	$f_{sl} = 1 - f_m$			
Lignin protection factor	$f(\text{Lig}) = \exp(-\alpha \times L_s)$	α	3.0	1.5
Climate control factor	$fA(T) = m \times \exp(0.095 \times T_{soil})$	m	1.0	0.5
	$fA(W) = \frac{1.0}{1.0+n\times\exp(-8.5\times w_{tat})}$	m	1.0	0.73
N mineralization and immobilization (C:N of AGMS)	$r_{AGML} = k1 \times N\% + k2$, where			
	$k1 = \frac{r_{max}-r_{min}}{0.019}$ and	γ_{max}, γ_{min}	22, 12	30, 8
	$k2 = \frac{20\times r_{max}-r_{min}}{19}$	γ_{max}, γ_{min}	22, 12	30, 8
	Belowground			
Partitioning of litter between BGDL and BGRL	$f_{ml} = c - d \times L/N$	c, d	none	0.74,0.015
N mineralization and immobilization (The ratio between C:N ratios of BGRL and BGDL)	$(C:N)_{BGRL}/(C:N)_{BGDL}$		none	3

four processes. The first process is the partitioning of leaf litter between metabolic material and structural material, which is crucial for the overall decay rate of leaf litter, N immobilization and N mineralization (Table 4). The original partitioning formulations for this process from *Parton et al.* [1987] and implemented in this study, were tested with several field data at time scales that range from 1 to 5 years [*Kirschbaum and Paul*, 2002]. Here we have further evaluated those formulations for a range of ecosystems and different climate regimes using LIDET data over 10 year time scale. The second process for optimization is the effect of [lignin] on decomposition (Table 4). According to *Moorhead et al.* [1999], the original formulation from *Parton et al.* [1987] describing the extent of lignin protection on the decay of structural material may be over estimated. The third process is the climatic (temperature and soil moisture) control on decomposition. The climatic dependence of litter and soil organic matter decomposition is a central feature of any ecosystem model [*Holland et al.*, 2000], and is highly variable [*Ise and Moorcroft*, 2006; *Giardina and Ryan*, 2000; *Knorr et al.*, 2005]. We calibrated the parameters involved in this process by utilizing the chosen data from LIDET, which represents a wide range of climate conditions (Table 4). The last process optimized is N mineralization and/or immobilization during decomposition. These processes controlling N content in decaying litter and soil mineral N availability, which are calibrated according to the parameters in the equations that are used to calculate C:N ratio of AGMS (Table 4).

[37] For belowground litter decomposition, the first process calibrated is the partitioning of root litter between BGDL and BGRL as applied by *Jain and Yang* [2005] based on the RothC model [*Jenkinson*, 1990]. The ratio of BGDL to BGRL is assumed to be 0.25 for all forests, 0.43 for savannas and 0.5 for deserts and tundra (Table 4) [*Jenkinson et al.*, 1991]. Here we assume that the partitioning of root litter between BGDL and BGRL is a function of root litter quality, i.e., [Lignin] and [N], as calibrated with LIDET data (Table 4). We have also calibrated N mineralization and/or immobilization during root decomposition by calibrating the proportionality between the C:N ratios of BGDL and that of BGRL to fit the model output with the observations (Table 4).

3.2.1. Best Fit Model Results for Aboveground Litter

[38] The model calibrated results for mass (C) of litter remaining and [N] of decaying litter are compared with LIDET observations in Figure 2. The decomposition rates for both high (1.98% N) and low-quality litter (0.38% N) based on analysis of mass remaining (Figure 2, left) show seasonal variations with faster loss during summer months and slower loss during winter months. In addition, it is shown that litter decomposes faster at warm moist sites compared to cold, dry sites for both litter types. This confirms the climatic controls on decomposition, and shows the highest mass loss rate at the tropical forest site, intermediate at the temperate forest, boreal forest, and grassland and lowest mass loss at the tundra site. In all cases, the modeled results are in agreement with observations from LIDET.

[39] Comparisons of calibrated [N] and LIDET observations across five biome types show that the model is able to capture the pattern of [N] changes during decomposition (Figure 2, right). Higher-quality litter decomposes faster than the lower-quality litter at all sites, indicating the control of litter quality on decomposition (Figure 2, right). In addition, the calibrated [N] of decomposing litter is consistent with patterns of mass loss, e.g., increasing [N] in the remaining litter with increasing mass loss. There is good agreement between the calibrated and the observed [N], however the agreement is generally higher for the high-quality litter than for lower-quality litter, probably due to large variability in the observational data of low-quality litter (Figure 2).

3.2.2. Best Fit Model Results for Belowground Litter

[40] The model calibrated results for mass remaining and [N] in decaying root litter compared to LIDET data is shown in Figure 3. Most variation in the quality of the root litter is attributed to different [lignin]; the [N] of the root litter considered here for calibration had little variation. Similarly to leaf litter, root litter also decomposes faster at

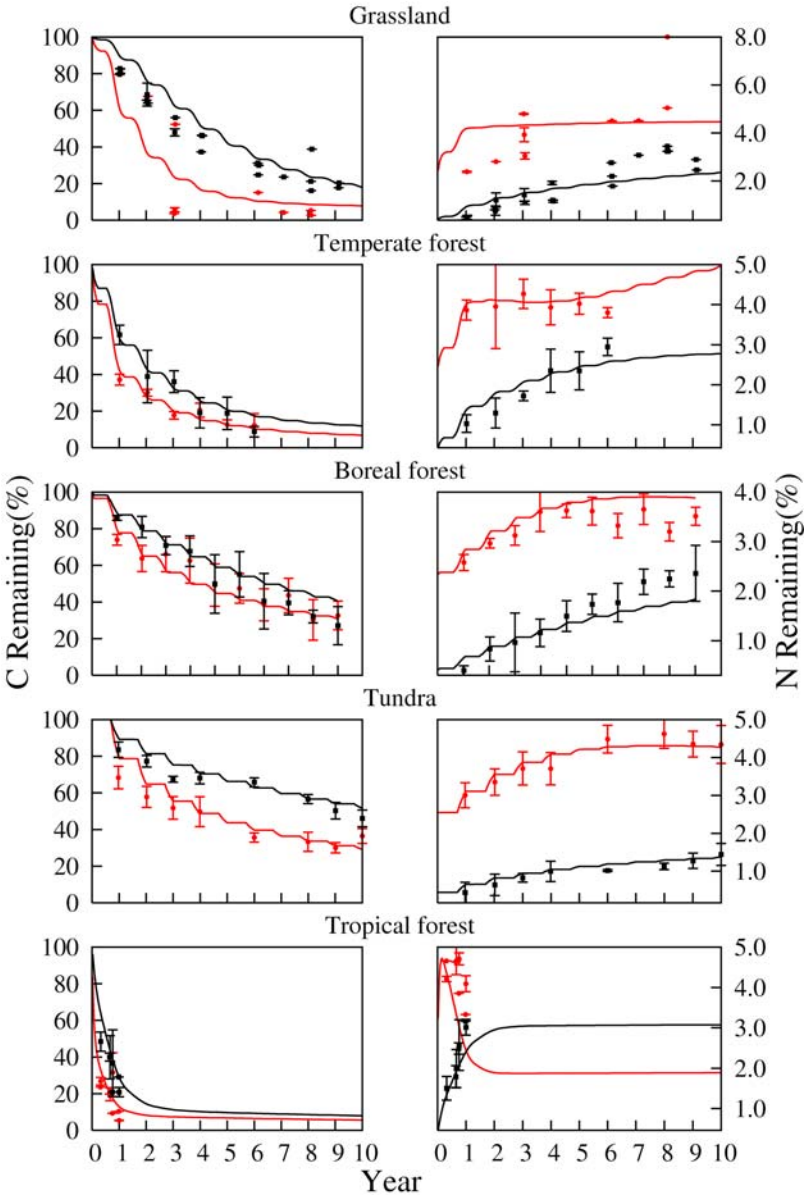

Figure 2. The comparison of observed and simulated (left) mass of carbon (C) remaining and (right) nitrogen (N) concentration of decaying leaf litter over 10 years at five sites representing five biomes. Red lines are the simulated decomposition of litter with 1.97% N and 10.8% Lignin; black lines are the simulated decomposition of litter with 0.38% N and 16.2% Lignin. Red symbols are mean observed decomposition of litter with 1.97% N and 10.8% Lignin; black symbols are mean observed decomposition of litter with 0.38% N and 16.2% Lignin; Error bars are one standard derivation of the observed mean.

warm moist sites and slower at dry cold sites (Figure 3, left) with good agreement between modeled results and observational data. Litter quality also contributes to percent mass remaining with higher-quality litter losing mass at a greater rate than low-quality litter. For example, high-quality tropical tree root litter with 0.76% N and 16.1% lignin decomposes faster than low-quality conifer tree root litter with 0.82% N and 34.9% lignin (Figure 3, left). The consistent pattern of lower [N] in low-quality litter compared to [N] of high-quality litter is captured by the model (Figure 3, right). The [N] of decaying root litter shows increasing trends in most biome types (Figure 3, right) again with good agreement between modeled results and LIDET data. The exception is the [N] of low-quality tundra root litter which is stable over time as compared to the high-quality litter which shows a slight increasing trend (Figure 3, right).

3.3. ISAM Evaluation

3.3.1. Aboveground Litter Decomposition

[41] A subset of LIDET data was used to evaluate the calibrated model. The model performance is evaluated

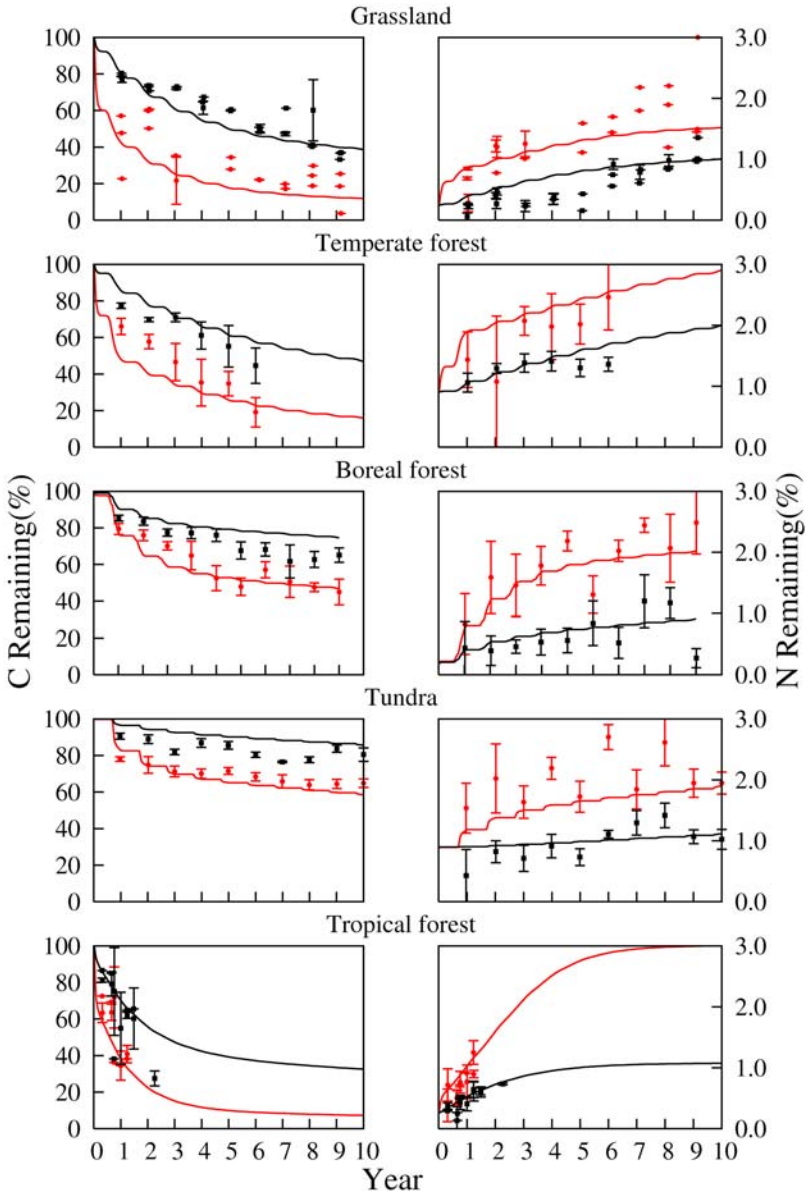

Figure 3. The comparison of observed and simulated (left) mass of carbon (C) remaining and (right) nitrogen (N) concentration of decaying root litter over 10 years at five sites representing five biomes. Red lines are the simulated decomposition of root litter with 0.76% N and 16.1% Lignin; black lines are the simulated decomposition of root litter with 0.82% N and 34.9% Lignin. Red symbols are mean observed decomposition of root litter with 0.76% N and 16.1% Lignin; black symbols are mean observed decomposition of root litter with 0.82% N and 34.9% Lignin; Error bars are one standard derivation of the observed mean.

through two standard statistical indices, e.g., correlation coefficient (r) and significance level (p). The model simulated litter mass remaining for the 10 year time period compared to field data is shown in Figure S1a. As indicated in Table S2, correlation between predicted and observed litter mass remaining are high ($r > 90\%$) and are statistically significant ($p < 0.01$) for almost all litter types and biomes. These comparisons clearly indicate that the model is capable of simulating mass loss patterns during long-term decomposition for a wide variety of litter types and climate regions. The model performs most successfully at tundra site and to a lesser extent at temperate and boreal forest sites with a slight overestimation of mass loss at earlier stages of decomposition (Figure S1a). The model slightly overestimates mass loss of decomposing litter at grassland sites. The possible reason for the overestimation of decomposition is that soil moisture instead of litter moisture was used in the model simulation. The moisture content in the litter layer could be much lower than that in soil, particularly for the grassland. Perhaps by overestimating litter moisture content,

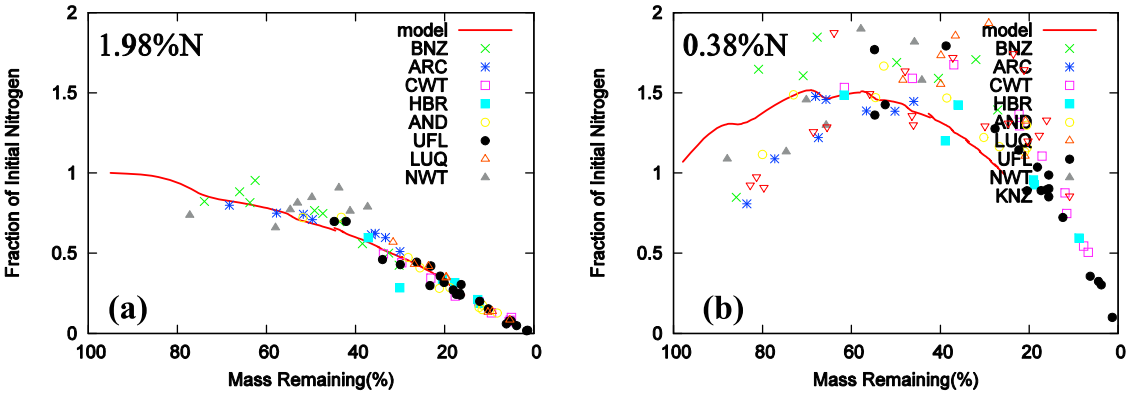

Figure 4. Fraction of initial litter N remaining as a function of the leaf litter mass remaining, with (a) high N litter with 1.98% N and (b) low N litter with 0.38% N. Data symbols shown in the graphs are the litter types for different biome sites defined in Table 3. The lines in the graphs are model simulations of the fraction of the initial N concentration as a function of litter mass remaining, averaged across all sites involved.

the decomposition rate of litter at the grassland site is overestimated. The [N] of decaying litter is shown in Figure S1b. The model simulations agree with the LIDET data as shown by the close 1:1 relationship between observed and predicted [N] in decaying litter (Figure S1b). It is clear that the model has the capacity to simulate N dynamics during decomposition in the long term for most of the combination of litter types and biomes. The low correlation between simulated and observed litter mass remaining and [N] in decaying litter in tropical forest and grassland (Tables S2 and S3) is probably caused by the bias in the observation data that is not accounted for by the model.

3.3.2. Belowground Litter Decomposition

[42] As described in section 3.1, root litter from a LIDET site with *Andropogon gerardii*, with 0.63% N and 10.5% lignin, was used to evaluate the model of belowground litter decomposition. In general, model simulated mass remaining and [N] of decaying litter for each biome site is in agreement with the LIDET data (Figures S2a and S2b). As with the simulation of aboveground litter decomposition, the model simulated values for the grassland site are higher than the median value of the observational data. As shown in Table S4, there is a good statistical correlation between predicted and the observed mass remaining and [N] dynamics during root litter decomposition.

3.3.3. Immobilization and Mineralization During Litter Decomposition

[43] Figure 4 shows model estimated variability in N immobilization and mineralization as a function of initial leaf [N] and mass remaining for highest and lowest initial [N] cases. It is important to note that there is a general pattern of increasing fraction of initial N in decomposing litter as the initial litter [N] decreases [*Parton et al.*, 2007]. Leaf litter with high initial [N] cases (1.98% N) shows no net immobilization during the decomposition process. The rate of N release decreases as the initial [N] decreases with the highest rate of net release for the 1.98% N case. The results are not shown here for two intermediate cases 1.02% N, 0.80% N. It is only in the initial [N] case of 0.38% N that a substantial amount of immobilization occurs (Figure 4). In this low initial [N] case, about 150% of the initial [N] is immobilized and the net N release starts only after about 60% of the mass has been lost. Model results are in agreement with LIDET data for the leaf litter with relatively high initial [N], but there is considerable discrepancy between modeled results and LIDET data for litter with low in initial [N], mainly because of very high variability in the LIDET data. Nonetheless, the model captures the overall N dynamics during decomposition at various biomes and over long time periods and is consistent with observations from other primary studies [*Aber and Melillo*, 1982; *Moorhead et al.*, 1999; *Parton et al.*, 2007]. In addition, the LIDET data and model results shown in Figure 4 support the conclusions of *Parton et al.* [2007] that the net N mineralization and immobilization during aboveground litter decomposition are dominantly controlled by the initial litter [N] and the mass remaining during decomposition.

[44] Modeled and observed root litter N follows a linear pattern of mass remaining and N released as soon as the decomposition of root litter begins (Figure 5) as microbial decomposers meet their N requirement directly from the litter. The modeled results are in agreement with observation, except for the initial stages of decomposition. Nevertheless, model captures the overall observed trend.

4. Steady-State Global Analysis

[45] The monthly temperature and precipitation data used in this study is the CRU TS 2.0 observation data set of the Tydall Center [*Mitchell and Jones*, 2005]. The mean temperature and precipitation for the period 1900–1920 and the 1765 atmospheric CO_2 concentration of 278 ppmv was used for the model spinup. Each grid cell is determined to have reached equilibrium when the annual fluxes of NPP, litter C production, and soil respiration differ by less than 10^{-3} Kg C m^{-2} yr^{-1} and when the fluxes of net N mineralization, litter

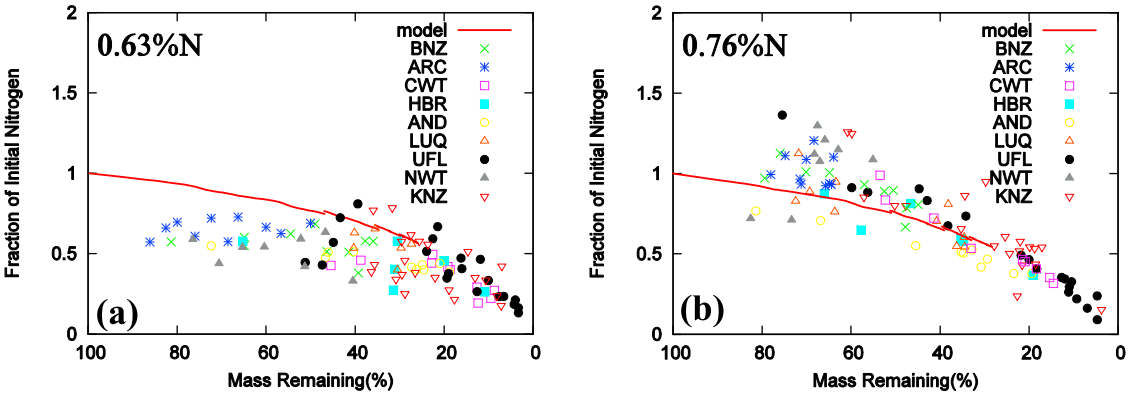

Figure 5. Fraction of original litter N remaining as a function of the root litter mass remaining, Data symbols shown in the graphs are two litter types: (a) 0.63% N litter and (b) 0.76% N litter for all sites, which represent different biomes as defined in Table 3. The lines in the graphs are the model simulations of the fraction of the initial N concentration as a function of litter mass remaining, averaged across all sites involved.

N production, and N uptake by vegetation differ by less than 10^{-5} Kg N m^{-2} yr^{-1}, and those of total N input (N deposition plus N fixation) and N output (denitrification plus leaching) differ by less than 10^{-5} Kg N m^{-2} yr^{-1}.

4.1. N Storage in Soils and Vegetation

[46] The mean model estimated steady state global distribution of soil N storage for the first 30 cm is 0.49 Kg N m^{-2}(65 Pg N) (Figure 6). Using the measured soil profile data for the upper 1 m, *Post et al.* [1985] and *Batjes* [1996] estimate global N amount in soils of about 95 PgN and 133–140 Pg N, respectively. Compared to these observed estimates, our modeled global mean value is quite reasonable considering that our estimates are for the first 30 cm soil, while the data-based estimates are for the upper 1 m soil.

[47] The density of organic N in soil modeled by ISAM in this study varies with biome type (Table S5), with highest soil organic N in tundra (1.24 Kg N m^{-2}), followed by temperate evergreen forest (0.90 Kg N m^{-2}), boreal forest (0.75 Kg N m^{-2}), and desert soil (0.06 Kg N m^{-2}). The higher N density in tundra is primarily due to the slow decomposition of organic matter caused by low temperatures, and water-saturated soils. At the same time, the C:N ratios for tropical forest soils are the lowest, due to the combined effects of higher temperature and precipitation in tropical forests contributing to higher litter decomposition. In contrast, in boreal forest and tundra higher C:N ratio combined with lower temperatures, contributes to comparatively slower decomposition rates (Table S5).

[48] In contrast to global distribution of soil N, vegetation N storage is highest in tropical evergreen forest and tropical deciduous forest (0.25–0.5 Kg N m^{-2}), followed by boreal forest (0.12–0.15 Kg N m^{-2}), tundra and desert (<0.03 Kg N m^{-2}) (Figure 7). The high-vegetation N storage in tropical forest is due to the high productivity and therefore strong N demand in these biomes. Our model estimated global distribution pattern of vegetation N are very similar to other global modeling studies, which suggest that most vegetation N is in tropical forest and the least is in tundra and desert [*Lin et al.*, 2000; *Xu-Ri and Prentice*, 2008]. Our model estimated global vegetation N storage value of 18 Pg N is largely in agreement with previously reported model estimates of 16 Pg N [*Lin et al.*, 2000].

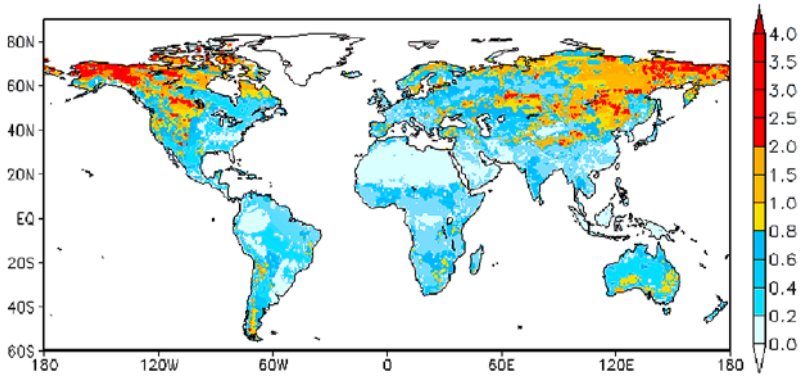

Figure 6. Model estimates of annual-mean N in soils (kg N m^{-2}).

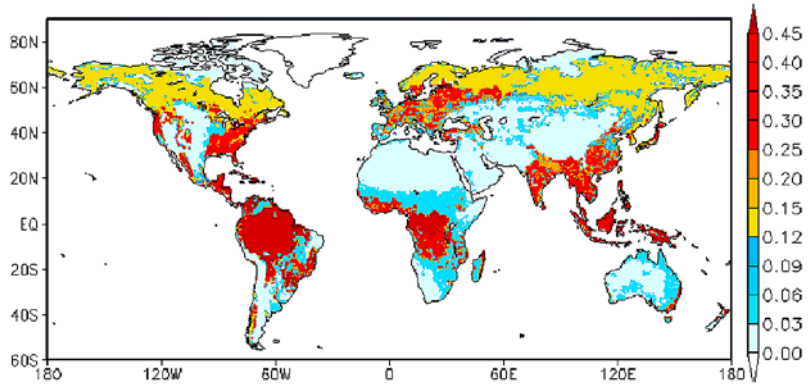

Figure 7. Model estimates of annual-mean N in vegetation (kg N m^{-2}).

4.2. N Uptake

[49] The spatial pattern of annual N uptake is highly correlated with climate patterns (Figure 8). In warm, moist tropical regions, where biomes such as tropical evergreen forest, tropical deciduous forest and savanna dominate, N uptake is highest (Figure 8). In cold, dry regions, where biomes such as boreal forest, tundra, and desert often dominate, N uptake tends to be lower. N uptake is the lowest in high latitudes where the cold, dry climate creates N limiting conditions and reduces N availability for plants. Global annual N uptake is 1.002 Pg N yr^{-1} (7.59 g N m^{-2} yr^{-1}), which is in good agreement with previous estimates of 1.084 Pg N yr^{-1} by *Xu-Ri and Prentice* [2008] and 1.073 Pg N yr^{-1} by *Melillo et al.* [1993].

4.3. N Leaching

[50] Figure 9 shows the model-estimated global distribution of annual N leaching from soil layers. The model effectively captured the control of soil moisture on rates of N leaching. Higher rates of N leaching are found in tropical regions and subtropical regions where soil moisture is higher (Figure 9). Soil N leaching in temperate zones is almost undetectable on a yearly average basis. Examination of model output on a seasonal time scale reveals the sensitivity of N leaching to periods of high water input such as during spring and summer in the temperate zones. Global nitrate leaching averaged about 0.47 g N m^{-2} yr^{-1} and is comparable to the 0.3 g N m^{-2} yr^{-1} estimate given by *Dickinson et al.* [2002].

5. Conclusions

[51] In this paper, the development of a global terrestrial model of N dynamics model and its coupling to the geographically explicit terrestrial C cycle component of ISAM is described. The N model incorporates all major processes governing the N cycle and the interaction with the C cycle in global terrestrial ecosystems. Decomposition is the major source of mineral N for biological activities in most terrestrial ecosystems [*Meentemeyer*, 1978; *Aerts*, 1997; *Parton et al.*, 2007]. By accounting for litter and SOM decomposition, the extended ISAM model structure effectively links N and C dynamics. The modified ISAM framework has been evaluated with a range of observations with a range of litter input rates, types, and climate conditions. This site-specific analysis demonstrates that ISAM is able to adequately capture N and C dynamics. The global patterns of vegetation and soil N, N uptake and N leaching are consistent with previous studies. The global distribution patterns of several N state variables such as mineral form N are not, however, available in the literature to evaluate the model performance. In order to improve the

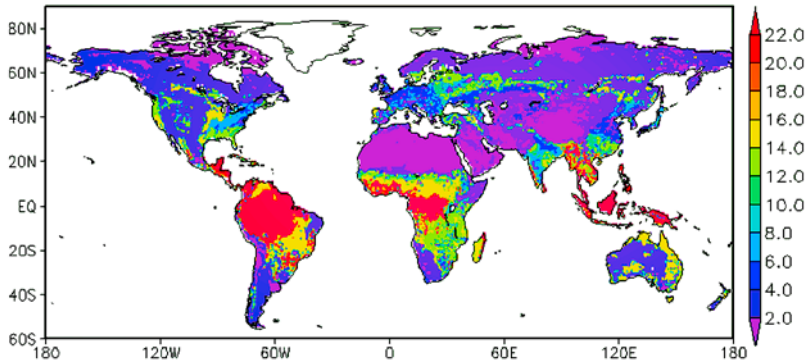

Figure 8. Model-estimated global distribution of the rate of annual N uptake (g N m^{-2} yr^{-1}).

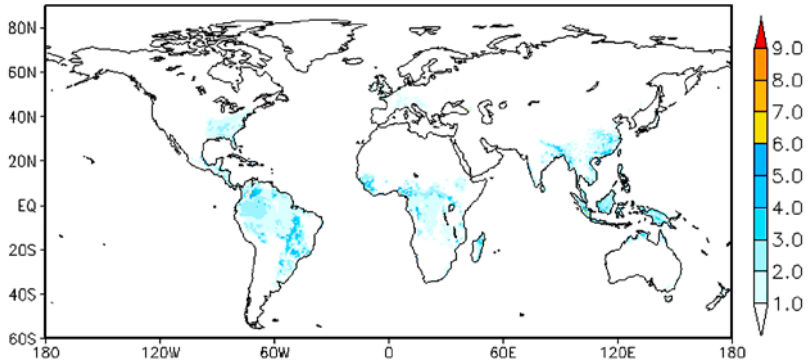

Figure 9. Model-estimated global distribution of the annual N leaching rate from soil layers (g N m^{-2} yr^{-1}).

accuracy of the model estimates additional experimental studies of C and N cycling at the global scale are required. Overall, inclusion of N dynamics and the good agreement between model simulation and measurements as presented in this study give increased confidence in the predictions of terrestrial C and N fluxes to and from the atmosphere. It further provides the framework for evaluating the interactive effects of C-N dynamics with environmental changes such as climate change, increasing atmospheric [CO_2], land cover and land use change and N deposition [*Jain et al.*, 2009].

[52] **Acknowledgments.** This research is supported in part by the U.S. National Aeronautics and Space Administration Land Cover and Land Use Change Program (NNX08AK75G), the Office of Science, U.S. Department of Energy (DOE DE-FG02-06ER64195), and Energy Biosciences Institute, University of Illinois.

References

Aber, J., and J. Melillo (1982), Nitrogen immobilization in decaying hardwood leaf litter as a function of initial nitrogen and lignin content, *Can. J. Bot.*, *60*(11), 2263–2269.

Aerts, R. (1997), Climate, leaf litter chemistry and leaf litter decomposition in terrestrial ecosystems: A triangular relationship, *Oikos*, *79*(3), 439–449, doi:10.2307/3546886.

Ainsworth, E. A., and S. P. Long (2005), What have we learned from 15 years of free-air CO_2 enrichment (FACE)? A meta-analytic review of the responses of photosynthesis, canopy properties and plant production to rising CO_2, *New Phytol.*, *165*, 351–371, doi:10.1111/j.1469-8137.2004.01224.x.

Azam, F., K. A. Malik, and M. I. Sajjad (1985), Transformations in soil and availability to plants of ^{15}N applied as inorganic fertilizer and legume residues, *Plant Soil*, *86*(1), 3–13, doi:10.1007/BF02185020.

Batjes, N. (1996), Total carbon and nitrogen in the soils of the world, *Eur. J. Soil Sci.*, *47*(2), 151–163, doi:10.1111/j.1365-2389.1996.tb01386.x.

Bauhus, J., and P. Khanna (1999), *The significance of microbial biomass in forest soils*, Going underground—Ecological studies in forest soils, edited by N. Rastin and J. Bauhus, Research Signpost, Trivandrum, India.

Berthelot, M., P. Friedlingstein, P. Ciais, J. L. Dufresne, and P. Monfray (2005), How uncertainties in future climate change predictions translate into future terrestrial carbon fluxes, *Global Change Biol.*, *11*(6), 959–970, doi:10.1111/j.1365-2486.2005.00957.x.

Bradbury, N. J., A. P. Whitmore, P. B. S. Hart, and D. S. Jenkinson (1993), Modelling the fate of nitrogen in crop and soil in the years following application of ^{15}N-labelled fertilizer to winter wheat, *J. Agric. Sci.*, *121*, 363–379, doi:10.1017/S0021859600085567.

Braswell, B., D. Schimel, E. Linder, and B. Moore III (1997), The response of global terrestrial ecosystems to interannual temperature variability, *Science*, *278*(5339), 870–873, doi:10.1126/science.278.5339.870.

Cao, L., and A. K. Jain (2005), An earth system model of intermediate complexity: Simulation of the role of ocean mixing parameterizations and climate change in estimated uptake for natural and bomb radiocarbon and anthropogenic CO_2, *J. Geophys. Res.*, *110*, C09002, doi:10.1029/2005JC002919.

Cao, L., and A. K. Jain (2008), Learning about the ocean carbon cycle from observational constraints and model simulation of multiple tracers, *Clim. Change*, *89*, 45–66, doi:10.1007/s10584-008-9421-1.

Cao, M., and F. I. Woodward (1998), Dynamic responses of terrestrial ecosystem carbon cycling to global climate change, *Nature*, *393*(6682), 249–252, doi:10.1038/30460.

Cleveland, C. C., A. R. Townsend, D. S. Schimel, H. Fisher, R. W. Howarth, L. O. Hedin, S. S. Perakis, E. F. Latty, J. C. Von Fischer, and A. Elseroad (1999), Global patterns of terrestrial biological nitrogen (N_2) fixation in natural ecosystems, *Global Biogeochem. Cycles*, *13*(2), 623–645, doi:10.1029/1999GB900014.

Corbeels, M., R. McMurtrie, D. Pepper, and A. O'Connell (2005), A process-based model of nitrogen cycling in forest plantations: Part I. Structure, calibration and analysis of the decomposition model, *Ecol. Modell.*, *187*(4), 426–448, doi:10.1016/j.ecolmodel.2004.09.005.

Cramer, W., et al. (1999), Comparing global models of terrestrial net primary productivity (NPP): Overview and key results, *Global Change Biol.*, *5*, 1–15, doi:10.1046/j.1365-2486.1999.00009.x.

Cramer, W., A. Bondeau, F. I. Woodward, I. C. Prentice, R. A. Betts, V. Brovkin, P. M. Cox, V. Fisher, J. A. Foley, and A. D. Friend (2001), Global response of terrestrial ecosystem structure and function to CO_2 and climate change: Results from six dynamic global vegetation models, *Global Change Biol.*, *7*(4), 357–373, doi:10.1046/j.1365-2486.2001.00383.x.

Curtis, P. S. (1996), A meta-analysis of leaf gas exchange and nitrogen in trees grown under elevated carbon dioxide, *Plant Cell Environ.*, *19*(2), 127–137, doi:10.1111/j.1365-3040.1996.tb00234.x.

DeLucia, E., D. Moore, and R. Norby (2005), Contrasting responses of forest ecosystems to rising atmospheric CO_2: Implications for the global C cycle, *Global Biogeochem. Cycles*, *19*, GB3006, doi:10.1029/2004GB002346.

Denman, K. L., et al. (2007), Couplings between changes in the climate system and biogeochemistry, in *Climate Change 2007: The Physical Science Basis. Contribution of Working Group I to the Fourth Assessment Report of the Intergovernmental Panel on Climate Change*, edited by S. Solomon et al., pp. 499–587, Cambridge Univ. Press, Cambridge, U. K.

Dickinson, R. E., et al. (2002), Nitrogen Controls on Climate Model Evapotranspiration, *J. Clim.*, *15*(3), 278–295, doi:10.1175/1520-0442(2002)015<0278:NCOCME>2.0.CO;2.

Finzi, A. C., D. J. P. Moore, E. H. DeLucia, J. Lichter, K. S. Hofmockel, R. B. Jackson, H. S. Kim, R. Matamala, H. R. McCarthy, and R. Oren (2006), Progressive nitrogen limitation of ecosystem processes under elevated CO_2 in a warm-temperate forest, *Ecology*, *87*(1), 15–25, doi:10.1890/04-1748.

Finzi, A. C., R. J. Norby, C. Calfapietra, A. Gallet-Budynek, B. Gielen, W. E. Holmes, M. R. Hoosbeek, C. M. Iversen, R. B. Jackson, and M. E. Kubiske (2007), Increases in nitrogen uptake rather than nitrogen-use efficiency support higher rates of temperate forest productivity under elevated CO_2, *Proc. Natl. Acad. Sci. U. S. A.*, *104*(35), 14,014, doi:10.1073/pnas.0706518104.

Friedlingstein, P., I. Fung, E. Holland, J. John, G. Brasseur, D. Erickson, and D. Schimel (1995), On the contribution of the biospheric CO_2 fertilization to the missing sink, *Global Biogeochem. Cycles*, *9*(4), 541–556, doi:10.1029/95GB02381.

Friedlingstein, P., G. Joel, C. Field, and I. Fung (1999), Toward an allocation scheme for global terrestrial carbon models, *Global Change Biol.*, *5*(7), 755–770, doi:10.1046/j.1365-2486.1999.00269.x.

Friedlingstein, P., P. Cox, R. Betts, L. Bopp, W. Von Bloh, V. Brovkin, P. Cadule, S. Doney, M. Eby, and I. Fung (2006), Climate–carbon cycle feedback analysis: Results from the C4MIP model intercomparison, *J. Clim.*, *19*(14), 3337–3353, doi:10.1175/JCLI3800.1.

Friend, A., A. Stevens, R. Knox, and M. Cannell (1997), A process-based, terrestrial biosphere model of ecosystem dynamics (Hybrid v3. 0), *Ecol. Modell.*, *95*(2–3), 249–287, doi:10.1016/S0304-3800(96)00034-8.

Galloway, J., F. Dentener, D. Capone, E. Boyer, R. Howarth, S. Seitzinger, G. Asner, C. Cleveland, P. Green, and E. Holland (2004), Nitrogen cycles: Past, present, and future, *Biogeochemistry*, *70*(2), 153–226, doi:10.1007/s10533-004-0370-0.

Gholz, H. L., D. A. Wedin, S. M. Smitherman, M. E. Harmon, and W. J. Parton (2000), Long-term dynamics of pine and hardwood litter in contrasting environments: Toward a global model of decomposition, *Global Change Biol.*, *6*(7), 751–765, doi:10.1046/j.1365-2486.2000.00349.x.

Giardina, C., and M. Ryan (2000), Evidence that decomposition rates of organic carbon in mineral soil do not vary with temperature, *Nature*, *404*(6780), 858–861, doi:10.1038/35009076.

Gill, R. A., H. W. Polley, H. B. Johnson, L. J. Anderson, H. Maherali, and R. B. Jackson (2002), Nonlinear grassland responses to past and future atmospheric CO_2, *Nature*, *417*(6886), 279–282, doi:10.1038/417279a.

Holland, E. A., J. C. Neff, A. R. Townsend, and B. McKeown (2000), Uncertainties in the temperature sensitivity of decomposition in tropical and subtropical ecosystems: Implications for models, *Global Biogeochem. Cycles*, *14*(4), 1137–1152, doi:10.1029/2000GB001264.

Hungate, B. A., P. D. Stiling, P. Dijkstra, D. W. Johnson, M. E. Ketterer, G. J. Hymus, C. R. Hinkle, and B. G. Drake (2004), CO_2 elicits long-term decline in nitrogen fixation, *Science*, *304*(5675), 1291, doi:10.1126/science.1095549.

Ise, T., and P. R. Moorcroft (2006), The global-scale temperature and moisture dependencies of soil organic carbon decomposition: An analysis using a mechanistic decomposition model, *Biogeochemistry*, *80*(3), 217–231, doi:10.1007/s10533-006-9019-5.

Ito, A. (2005), Climate-related uncertainties in projections of the twenty-first century terrestrial carbon budget: Off-line model experiments using IPCC greenhouse-gas scenarios and AOGCM climate projections, *Clim. Dyn.*, *24*(5), 435–448, doi:10.1007/s00382-004-0489-7.

Jain, A. K., and X. Yang (2005), Modeling the effects of two different land cover change data sets on the carbon stocks of plants and soils in concert with CO_2 and climate Change, *Global Biogeochem. Cycles*, *19*, GB2015, doi:10.1029/2004GB002349.

Jain, A. K., H. S. Kheshgi, M. I. Hoffert, and D. J. Wuebbles (1995), Distribution of radiocarbon as a test of global carbon cycle models, *Global Biogeochem. Cycles*, *9*, 153–166, doi:10.1029/94GB02394.

Jain, A. K., H. S. Kheshgi, and D. J. Wuebbles (1996), A globally aggregated reconstruction of cycles of carbon and its isotopes, *Tellus, Ser. B*, *48*(4), 583–600, doi:10.1034/j.1600-0889.1996.t01-1-00012.x.

Jain, A. K., Z. Tao, X. Yang, and C. Gillespie (2006), Estimates of global biomass burning emissions for reactive greenhouse gases (CO, NMHCs, and NOx) and CO_2, *J. Geophys. Res.*, *111*, D06304, doi:10.1029/2005JD006237.

Jain, A. K., X. Yang, H. Kheshgi, A. D. McGuire, W. Post, and D. Kicklighter (2009), Nitrogen attenuation of terrestrial carbon cycle response to global environmental factors, *Global Biogeochem. Cycles*, *23*, GB4028, doi:10.1029/2009GB003519.

Jenkinson, D. (1990), The turnover of organic carbon and nitrogen in soil, *Philos. Trans. R. Soc. London, Ser. B*, *329*(1255), 361–367, doi:10.1098/rstb.1990.0177.

Jenkinson, D. S., D. E. Adams, and A. Wild (1991), Model estimates of CO_2 emissions from soil in response to global warming, *Nature*, *351*(6322), 304–306.

Kheshgi, H. S., A. K. Jain, and D. J. Wuebbles (1996), Accounting for the missing carbon-sink with the CO_2-fertilization effect, *Clim. Change*, *33*(1), 31–62, doi:10.1007/BF00140512.

King, A. W., W. R. Emanuel, S. D. Wullschleger, and W. M. Post (1995), In search of the missing carbon sink: A model of terrestrial biospheric response to land-use change and atmospheric CO_2, *Tellus, Ser. B*, *47*(4), 501–519, doi:10.1034/j.1600-0889.47.issue4.9.x.

King, A. W., W. M. Post, and S. D. Wullschleger (1997), The potential response of terrestrial carbon storage to changes in climate and atmospheric CO_2, *Clim. Change*, *35*(2), 199–227, doi:10.1023/A:1005317530770.

Kirschbaum, M. U. F., and K. I. Paul (2002), Modelling C and N dynamics in forest soils with a modified version of the CENTURY model, *Soil Biol. Biochem.*, *34*(3), 341–354, doi:10.1016/S0038-0717(01)00189-4.

Knorr, W., I. Prentice, J. House, and E. Holland (2005), Long-term sensitivity of soil carbon turnover to warming, *Nature*, *433*(7023), 298–301, doi:10.1038/nature03226.

Koch, G. W., and H. A. Mooney (1996), Response of terrestrial ecosystems to elevated CO_2: A synthesis and summary, in *Carbon Dioxide and Terrestrial Ecosystems*, pp. 415–429, edited by G. W. Koch and H. A. Mooney, Academic, San Diego, Calif.

Körner, C. (2000), Biosphere responses to CO_2 enrichment, *Ecol. Appl.*, *10*(6), 1590–1619.

Lin, B. L., A. Sakoda, R. Shibasaki, N. Goto, and M. Suzuki (2000), Modelling a global biogeochemical nitrogen cycle in terrestrial ecosystems, *Ecol. Modell.*, *135*(1), 89–110, doi:10.1016/S0304-3800(00)00372-0.

Long, S. P., E. A. Ainsworth, A. Rogers, and D. R. Ort (2004), Rising atmospheric carbon dioxide: Plants FACE the future, *Annu. Rev. Plant Biol.*, *55*(1), 591–628, doi:10.1146/annurev.arplant.55.031903.141610.

Long-Term Intersite Decomposition Experiment Team (LIDET) (1995), Meeting the challenge of long-term, broad-scale ecological experiments, *LTER Publ. 19*, 23 pp., U.S. LTER Network Off., Seattle, Wash.

Luo, Y., et al. (2004), Progressive nitrogen limitation of ecosystem responses to rising atmospheric carbon dioxide, *BioScience*, *54*(8), 731–739, doi:10.1641/0006-3568(2004)054[0731:PNLOER]2.0.CO;2.

McGuire, A. D., J. Melillo, L. Joyce, D. Kicklighter, A. Grace, B. Moore III, and C. Vorosmarty (1992), Interactions between carbon and nitrogen dynamics in estimating net primary productivity for potential vegetation in North America, *Global Biogeochem. Cycles*, *6*(2), 101–124, doi:10.1029/92GB00219.

McGuire, A. D., J. Melillo, D. Kicklighter, and L. Joyce (1995), Equilibrium responses of soil carbon to climate change: Empirical and process-based estimates, *J. Biogeogr.*, *22*, 785–796.

McGuire, A., S. Sitch, J. Clein, R. Dargaville, G. Esser, J. Foley, M. Heimann, F. Joos, J. Kaplan, and D. Kicklighter (2001), Carbon balance of the terrestrial biosphere in the twentieth century: Analyses of CO_2, climate, and land use effects with four process-based ecosystem models, *Global Biogeochem. Cycles*, *15*(1), 183–206, doi:10.1029/2000GB001298.

Meentemeyer, V. (1978), Macroclimate and lignin control of litter decomposition rates, *Ecology*, *59*(3), 465–472, doi:10.2307/1936576.

Melillo, J. M., A. D. McGuire, D. W. Kicklighter, B. Moore, C. J. Vorosmarty, and A. L. Schloss (1993), Global climate change and terrestrial net primary production, *Nature*, *363*, 234–240, doi:10.1038/363234a0.

Mitchell, T. D., and P. D. Jones (2005), An improved method of constructing a database of monthly climate observations and associated high resolution grids, *Int. J. Climatol.*, *25*, 693–712.

Mooney, H. A., J. Canadell, F. S. Chapin III, J. R. Ehleringer, C. Körner, R. E. McMurtrie, W. J. Parton, L. F. Pitelka, and E. D. Schulze (1999), Ecosystem physiology responses to global change, in *Implications of Global Change for Natural and Managed Ecosystems. A Synthesis of GCTE and Related Research*, *IGBP Book Ser.*, vol. 4, edited by B. H. Walker et al., pp. 141–189, Cambridge Univ. Press, Cambridge, U. K.

Moorhead, D., and J. Reynolds (1991), A general model of litter decomposition in the northern Chihuahuan Desert, *Ecol. Modell.*, *56*(1–4), 197–219.

Moorhead, D., W. Currie, E. Rastetter, W. Parton, and M. Harmon (1999), Climate and litter quality controls on decomposition: An analysis of modeling approaches, *Global Biogeochem. Cycles*, *13*(2), 575–590, doi:10.1029/1998GB900014.

Mosier, A., J. Morgan, J. King, D. LeCain, and D. Milchunas (2002), Soil-atmosphere exchange of CH 4, CO 2, NO x, and N 2 O in the Colorado shortgrass steppe under elevated CO 2, *Plant Soil*, *240*(2), 201–211, doi:10.1023/A:1015783801324.

Norby, R. J., and M. F. Cotrufo (1998), Global change: A question of litter quality, *Nature*, *396*, 17–18.

Norby, R. J., S. D. Wullschleger, C. A. Gunderson, D. W. Johnson, and R. Ceulemans (1999), Tree responses to rising CO_2: Implications for the future forest, *Plant Cell Environ.*, *22*, 683–714.

Norby, R. J., M. F. Cotrufo, P. Ineson, E. G. O'Neill, and J. G. Canadell (2001), Elevated CO_2, litter quality, and decomposition: A synthesis, *Oecologia*, *127*, 153–165, doi:10.1007/s004420000615.

Norby, R. J., E. H. DeLucia, B. Gielen, C. Calfapietra, C. P. Giardina, J. S. King, J. Ledford, H. R. McCarthy, D. J. P. Moore, and R. Ceulemans (2005), Forest response to elevated CO_2 is conserved across a broad range of productivity, *Proc. Natl. Acad. Sci. U. S. A.*, *102*(50), 18,052–18,056, doi:10.1073/pnas.0509478102.

Nowak, R. S., D. S. Ellsworth, and S. D. Smith (2004), Functional responses of plants to elevated atmospheric CO_2: Do photosynthetic and productivity data from FACE experiments support early predictions?, *New Phytol.*, *162*, 253–280, doi:10.1111/j.1469-8137.2004.01033.x.

Oren, R., D. S. Ellsworth, K. H. Johnsen, N. Phillips, B. E. Ewers, C. Maier, K. V. R. Schafer, H. McCarthy, G. Hendrey, and S. G. McNulty (2001), Soil fertility limits carbon sequestration by forest ecosystems in a CO_2-enriched atmosphere, *Nature*, *411*(6836), 469–472, doi:10.1038/35078064.

Parton, W., D. Schimel, C. Cole, and D. Ojima (1987), Analysis of factors controlling soil organic matter levels in Great Plains grasslands, *Soil Sci. Soc. Am. J.*, *51*(5), 1173–1179.

Parton, W., D. Schimel, D. Ojima, and C. Vernon Cole (1994), A general model for soil organic matter dynamics: Sensitivity to litter chemistry, texture and management, in *Quantitative Modeling of Soil Forming Processes*, *SSSA Spec. Publ.*, *39*, 147–167.

Parton, W., W. L. Silver, I. C. Burke, L. Grassens, M. E. Harmon, W. S. Currie, J. Y. King, E. C. Adair, L. A. Brandt, and S. C. Hart (2007), Global-scale similarities in nitrogen release patterns during long-term decomposition, *Science*, *315*(5810), 361–364, doi:10.1126/science.1134853.

Pastor, J., and W. Post (1985), Development of a linked forest productivity-soil process model, *ORNL TM-9519*, Oak Ridge National Lab., TN, USA.

Paul, K., and P. Polglase (2004), Prediction of decomposition of litter under eucalypts and pines using the FullCAM model, *For. Ecol. Manage.*, *191*(1–3), 73–92, doi:10.1016/j.foreco.2003.11.007.

Peterson, A. G., J. T. Ball, Y. I. Luo, C. B. Field, P. B. Reich, P. S. Curtis, K. L. Griffin, C. A. Gunderson, R. J. Norby, and D. T. Tissue (1999), The photosynthesis-leaf nitrogen relationship at ambient and elevated atmospheric carbon dioxide: A meta-analysis, *Global Change Biol.*, *5*(3), 331–346, doi:10.1046/j.1365-2486.1999.00234.x.

Poorter, H. (1993), Interspecific variation in the growth response of plants to an elevated ambient CO_2 concentration, *Plant Ecol.*, *104*(1), 77–97, doi:10.1007/BF00048146.

Post, W. M., J. Pastor, P. J. Zinke, and A. G. Stangenberger (1985), Global patterns of soil nitrogen storage, *Nature*, *317*(6038), 613–616, doi:10.1038/317613a0.

Post, W. M., A. W. King, and S. D. Wullschleger (1997), Historical variations in terrestrial biospheric carbon storage, *Global Biogeochem. Cycles*, *11*, 99–110, doi:10.1029/96GB03942.

Potter, C. S., and S. A. Klooster (1997), Global model estimates of carbon and nitrogen storage in litter and soil pools: Response to changes in vegetation quality and biomass allocation, *Tellus, Ser. B*, *49*(1), 1–17, doi:10.1034/j.1600-0889.49.issue1.1.x.

Prentice, C., G. Farquhar, M. Fasham, M. Goulden, M. Heimann, V. Jaramillo, H. Kheshgi, C. L. Que're', R. Scholes, and D. Wallace (2001), The carbon cycle and atmospheric CO_2, in *Climate Change 2001: The Scientific Basis: Contribution of WGI to the Third Assessment Report of the IPCC*, edited by J. T. Houghton et al., pp. 183–237, Cambridge Univ. Press, New York.

Raich, J., E. Rastetter, J. Melillo, D. W. Kicklighter, P. A. Steudler, B. Peterson, A. Grace, B. Moore III, and C. Vorosmarty (1991), Potential net primary productivity in South America: Application of a global model, *Ecol. Appl.*, *1*(4), 399–429, doi:10.2307/1941899.

Reich, P., J. Knops, D. Tilman, J. Craine, D. Ellsworth, M. Tjoelker, T. Lee, D. Wedin, S. Naeem, and D. Bahauddin (2001), Plant diversity enhances ecosystem responses to elevated CO_2 and nitrogen deposition, *Nature*, *410*(6830), 809–812, doi:10.1038/35071062.

Reich, P. B., B. A. Hungate, and Y. Luo (2006), Carbon-nitrogen interactions in terrestrial ecosystems in response to rising atmospheric carbon dioxide, *Annu. Rev. Ecol. Evol. Syst.*, *37*, 611–636.

Rustad, L., J. Campbell, G. Marion, R. Norby, M. Mitchell, A. Hartley, J. Cornelissen, and J. Gurevitch (2001), A meta-analysis of the response of soil respiration, net nitrogen mineralization, and aboveground plant growth to experimental ecosystem warming, *Oecologia*, *126*(4), 543–562, doi:10.1007/s004420000544.

Schimel, D. S., B. Braswell, R. McKeown, D. Ojima, W. Parton, and W. Pulliam (1996), Climate and nitrogen controls on the geography and timescales of terrestrial biogeochemical cycling, *Global Biogeochem. Cycles*, *10*, 677–692, doi:10.1029/96GB01524.

Shaver, G. R., J. Canadell, F. Chapin III, J. Gurevitch, J. Harte, G. Hengy, P. Ineson, S. Jonasson, J. Melillo, and L. Pitelka (2000), Global warming and terrestrial ecosystems: A conceptual framework for analysis, *BioScience*, *50*(10), 871–882, doi:10.1641/0006-3568(2000)050[0871:GWATEA]2.0.CO;2.

Smith, J. E., L. Heath, and J. Jenkins (2003), Forest volume-to-biomass models and estimates of mass for live and standing dead trees of U.S. forests, *Gen. Tech. Rep. NE-298*, Newtown Square, Pa. U.S. Dept. of Agric., For. Serv., Northeastern Res. Sta. 57.

Smith, P., J. Smith, D. Powlson, W. McGill, J. Arah, O. Chertov, K. Coleman, U. Franko, S. Frolking, and D. Jenkinson (1997), A comparison of the performance of nine soil organic matter models using datasets from seven long-term experiments, *Geoderma*, *81*(1–2), 153–225, doi:10.1016/S0016-7061(97)00087-6.

Sokolov, A. P., D. W. Kicklighter, J. M. Melillo, B. S. Felzer, C. A. Schlosser, and T. W. Cronin (2008), Consequences of considering carbon-nitrogen interactions on the feedbacks between climate and the terrestrial carbon cycle, *J. Clim.*, *21*(15), 3776–3796, doi:10.1175/2008JCLI2038.1.

Stott, D. E., G. Kassim, W. M. Jarrell, J. P. Martin, and K. Haider (1983), Stabilization and incorporation into biomass of specific plant carbons during biodegradation in soil, *Plant Soil*, *70*(1), 15–26, doi:10.1007/BF02374746.

Tao, Z., and A. K. Jain (2005), Modeling of global biogenic emissions for key indirect greenhouse gases and their response to atmospheric CO_2 increases and changes in land cover and climate, *J. Geophys. Res.*, *110*, D21309, doi:10.1029/2005JD005874.

Thornley, J. H. M., and M. G. R. Cannell (2000), Dynamics of mineral N availability in grassland ecosystems under increased [CO_2]: Hypotheses evaluated using the Hurley Pasture Model, *Plant Soil*, *224*(1), 153–170, doi:10.1023/A:1004640327512.

Thornton, P. E., J.-F. Lamarque, N. A. Rosenbloom, and N. M. Mahowald (2007), Influence of carbon-nitrogen cycle coupling on land model response to CO_2 fertilization and climate variability, *Global Biogeochem. Cycles*, *21*, GB4018, doi:10.1029/2006GB002868.

Thornton, P., S. Doney, K. Lindsay, J. Moore, N. Mahowald, J. Randerson, I. Fung, J. Lamarque, J. Feddema, and Y. Lee (2009), Carbon-nitrogen interactions regulate climate–carbon cycle feedbacks: Results from an atmosphere-ocean general circulation model, *Carbon*, *6*, 3303–3354.

Tian, H., J. Melillo, D. Kicklighter, A. McGuire, and J. Helfrich (1999), The sensitivity of terrestrial carbon storage to historical climate variability and atmospheric CO_2 in the United States, *Tellus, Ser. B*, *51*(2), 414–452, doi:10.1034/j.1600-0889.1999.00021.x.

White, M. A., P. E. Thornton, S. W. Running, and R. R. Nemani (2000), Parameterization and sensitivity analysis of the BIOME–BGC terrestrial ecosystem model: Net primary production controls, *Earth Interact.*, *4*, 1–85, doi:10.1175/1087-3562(2000)004<0003:PASAOT>2.0.CO;2.

Xu-Ri, , and I. C. Prentice (2008), Terrestrial nitrogen cycle simulation with a dynamic global vegetation model, *Global Change Biol.*, *14*(8), 1745–1764, doi:10.1111/j.1365-2486.2008.01625.x.

Zak, D., W. Holmes, A. Finzi, R. Norby, and W. Schlesinger (2003), Soil nitrogen cycling under elevated CO_2: A synthesis of forest face experiments, *Ecol. Appl.*, *13*(6), 1508–1514, doi:10.1890/03-5055.

Zhou, J. L., A. L. Tits, and C. T. Lawrence (1997), User's Guide for FFSQP Version 3.7: A Fortran Code for Solving Optimization Programs, Possibly Minimax, with General Inequality Constraints and Linear Equality Constraints, Generating Feasible Iterates, *Tech. Rep. SRC-TR-92-107r5*, Inst. for Syst. Res., Univ. of Md., College Park, Md.

A. K. Jain, V. Wittig, and X. Yang, Department of Atmospheric Sciences, University of Illinois at Urbana-Champaign, Urbana, IL 61801, USA. (jain1@uiuc.edu)

W. Post, Oak Ridge National Laboratory, Oak Ridge, TN 37831, USA.